Bachelor's thesis

NTNU
Norwegian University of Science and Technology
Faculty of Engineering
Department of Energy and Process Engineering

Jo Emil Spakmo
Magnus Langelid

On Flywheel Batteries

Om Roterende Masse Batterier

Bachelor's thesis in Renewable Energy
Supervisor: Reidar Kristoffersen
May 2023

NTNU
Norwegian University of
Science and Technology

Jo Emil Spakmo
Magnus Langelid

On Flywheel Batteries

Om Roterende Masse Batterier

Bachelor's thesis in Renewable Energy
Supervisor: Reidar Kristoffersen
May 2023

Norwegian University of Science and Technology
Faculty of Engineering
Department of Energy and Process Engineering

NTNU
Norwegian University of
Science and Technology

NTNU
Institutt for energi- og prosessteknikk

Bacheloroppgave

Oppgavens tittel: Om Roterende Masse Batterier **Project title (ENG):** On Flywheel Batteries	**Gitt dato:** 21.11.2022 **Innleveringsdato:** 22.05.2023 **Antall sider rapport / sider vedlagt:** 57/26
Gruppedeltakere: Jo Emil Spakmo Magnus Langelid	**Veileder:** Reidar Kristoffersen **Prosjektnummer:** BIFOREN23-22
Oppdragsgiver: Norges teknisk-naturvitenskapelige universitet	**Kontaktperson hos oppdragsgiver:** Jacob J. Lamb

Fritt tilgjengelig: ☒

Tilgjengelig etter avtale med oppdragsgiver: ☐

Rapporten frigitt etter: 22.05.2023

Gruppedeltakere signaturer:

Emil Spakmo

Magnus Langelid

Preface

This is a collaborative bachelor thesis between Jo Emil Spakmo and Magnus Langelid as a final project at the Renewable Energy Bachelor's Degree Programme at the Norwegian University of Science and Technology. The thesis investigates flywheel energy storage and its uses. It combines knowledge in fields such as mechanics, electrical machines and control engineering which is obtained through courses at the university and through research with this project.

The students would like to thank all the professors at the study programme and especially Reidar Kristoffersen for being an excellent supervisor.

Emil Spakmo

Jo Emil Spakmo

Magnus Langelid

Magnus Langelid

Date: 22.05.2023

Abstract

Energy storage systems improves electrical system efficiency during supply and demand imbalances, enhancing network stability and quality. They mitigate the intermittency of renewable generation and provide system flexibility. Flywheel energy storage systems (FESS) have attracted considerable interest due to their advantages: high cycle and operational life, efficient energy conversion, high power density, low environmental impact, and scalable energy storage capacity reaching megajoule levels.

This paper begins with a literature review of the FESS. It then explores the various applications and primary uses of FESS. Additionally, simulations of different scenarios utilizing FESS, along with the underlying theory, are presented.

Finally, the paper concludes with a comprehensive discussion, summarizing the findings, and providing recommendations for future research. The primary findings indicate that the FESS is most effective in situations requiring rapid charging, particularly with short time intervals between charges. Furthermore, it was observed that a higher moment of inertia results in slower charging and discharging of the FESS. Additionally, the study highlights the impact of different types of electric machines on the operation of the FESS, specifically in terms of charge and discharge times.

Sammendrag

Energilagringssystemer forbedrer effektiviteten i elektriske systemer under ubalanser mellom tilbud og etterspørsel, og bidrar til å øke nettverkets stabilitet og kvalitet. De reduserer ujevnheten i fornybar energiproduksjon og gir systemet fleksibilitet. Roterende masse baserte energilagringssystemer (FESS) har skapt betydelig interesse på grunn av deres fordeler: lang levetid, effektiv energiomforming, høy effekttetthet, lav miljøpåvirkning og skalerbar energilagringskapasitet på nivåer opp til megajoule.

Denne rapporten begynner med en litteraturstudie av FESS. Deretter utforsker den ulike bruksområder og hovedanvendelser av FESS. I tillegg presenteres simuleringer av ulike scenarier som bruker FESS, sammen med den underliggende teorien.

Avslutningsvis diskuteres funnene grundig, oppsummeres, og det gis anbefalinger for fremtidig forskning. De viktigste funnene indikerer at FESS er mest effektiv i situasjoner som krever rask lading, spesielt med korte tidsintervaller mellom ladingene. Videre ble det observert at et høyere treghetsmoment fører til tregere lading og utlading av FESS. Studien fremhever også hvordan ulike typer elektriske maskiner påvirker driften av FESS, spesielt med tanke på ladetider og utladningstider.

List of terms

Block diagram	A diagram of a system where its parts are represented by blocks and are connected by lines that shows their relationships.
Bode plot	A plot where the amplitude and phase of a transfer function is plotted versus frequencies.
Closed feedback loop	A control loop where the output signal is fed back to the input.
Depth of discharge	The percentage of the energy storage's capacity which is removed from the battery with regard to its fully charged state.
Electric machine	Electric device that functions as a generator and a motor.
Equivalent circuit	An electric circuit which describes the voltages, currents and resistances in an electric machine.
Open loop	A control loop where the output signal does not feed back to the input.
Ragone plot	A plot which compares peak power output and energy storage capacity per mass.
Round trip efficiency	Total efficiency of charging, storing and discharging of system.
Spin out time	The time it takes for the flywheel to lose all its stored energy due to losses.
Thevenin equivalent circuit	The circuit between to terminals replaced with a voltage source and an impedance in series to make it easier to analyze.
Transfer function	A function that describes the output signal from a system or component when an input signal is applied.

List of abbreviations

AC	Alternating current
DC	Direct current
FESS	Flywheel energy storage system
FW	Flywheel rotor, bearings, housing, and ancillaries
IM	Induction machine
MG	Motor/generator
MGPE	Motor/generator with power electronics, including a grid tied inverter
PMSM	Permanent magnetic synchronous machine
PID	Proportional integral derivative
PV	Photovoltaic
VRM	Variable reluctance machine

List of symbols

	Latin symbols
A	Air drag coefficient [-]
B	Eddy-current coefficient [-]
C	Hysteresis coefficient [-]
E	Energy [J]
e_m	Specific energy [J/kg]
e_v	Energy density [J/m^3]
f	Frequency [Hz]
Gm	Gain margin [dB]
h	Transfer function [-]
h_0	Open loop transfer function [-]
h_0^*	Open loop transfer function without controller [-]
I	Moment of inertia [kg$\cdot$ m^2]
K	Shape factor [-]
K_p	Proportional gain [-]
L	Angular momentum [kg$\cdot$ m$^2/s$]
m	Mass [kg]
n	Rotational speed [RPM]
n_s	Synchronous speed [RPM]
P	Power [W]
Pm	Phase margin [°]
R	Resistance [-]
s	Slip [-]
t	Time [s]
T_d	Differentiation time [s]

T_i	Integration time [s]

Greek symbols

ρ	Density [kg/m^3]
σ	Tensile strength [Pa]
τ	Torque [Nm]
ω	Angular velocity [rad/s]
ω_w	Desired frequency [rad/s]
η	Efficiency [-]

Contents

List of Figures

List of Tables

1 Introduction

The World's energy practice is in a transition. The topic of clean and green energy has grown to a major concern and center of attention, both for governments, industries and individuals. Sectors, industries and processes are being electrified to reduce their carbon footprint. This causes the electricity demand to increase [36]. Figure 1.1b shows three models for future electricity demands for different sectors. To meet the increasing electricity demand, in a green manner, there needs to be an increase in renewable energy production. Although production from many renewable energy sources can be predicted through tools such as weather forecasts, their production cannot be controlled and regulated as easily as many fossil sources. This causes complications where the energy produced does not match the power demand. As figure 1.1a illustrates, renewable energy production has increased substantially the last 10 years [44].

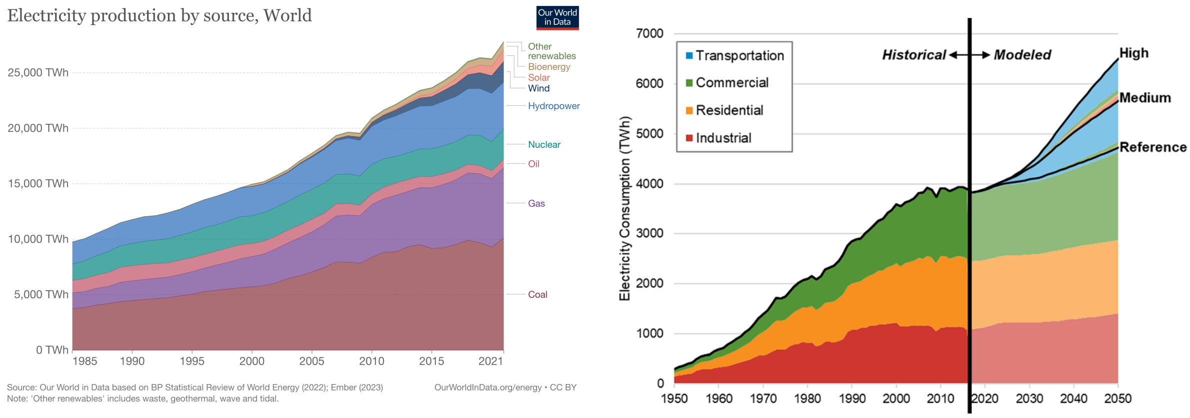

(a) World's energy production by source [44].

(b) Future energy demand by sector [36].

Figure 1.1: Energy production and future energy demand.

1.1 Motivation

Energy storage is an important solution to several of the problems the energy transition brings along. Firstly, storing excess energy from renewable energy sources when production is high and demand is low is essential for obtaining a sustainable energy system. Another application where energy storage can contribute to the energy transition is to relieve the power grid at high loads. Today's power grid is not dimensioned for the futures energy demands and the power peaks that comes with it [55]. An additional use where energy storage solutions is necessary is in the transportation sector. As shown in figure 1.1b, the electricity demand for the transportation sector will increase substantially and thus the need for mobile energy storage solution will also increase.

Energy storage exists in many different forms: Electrochemical which includes lithium-ion and lead-acid batteries, thermal, electrical, hydrogen based (chemical) and lastly mechanical energy storage [27]. Mechanical energy storage systems include pumped hydro energy storage, compressed air energy storage and flywheel energy storage. Figure 1.2 shows different energy storage systems and their properties in a Ragone plot [21].

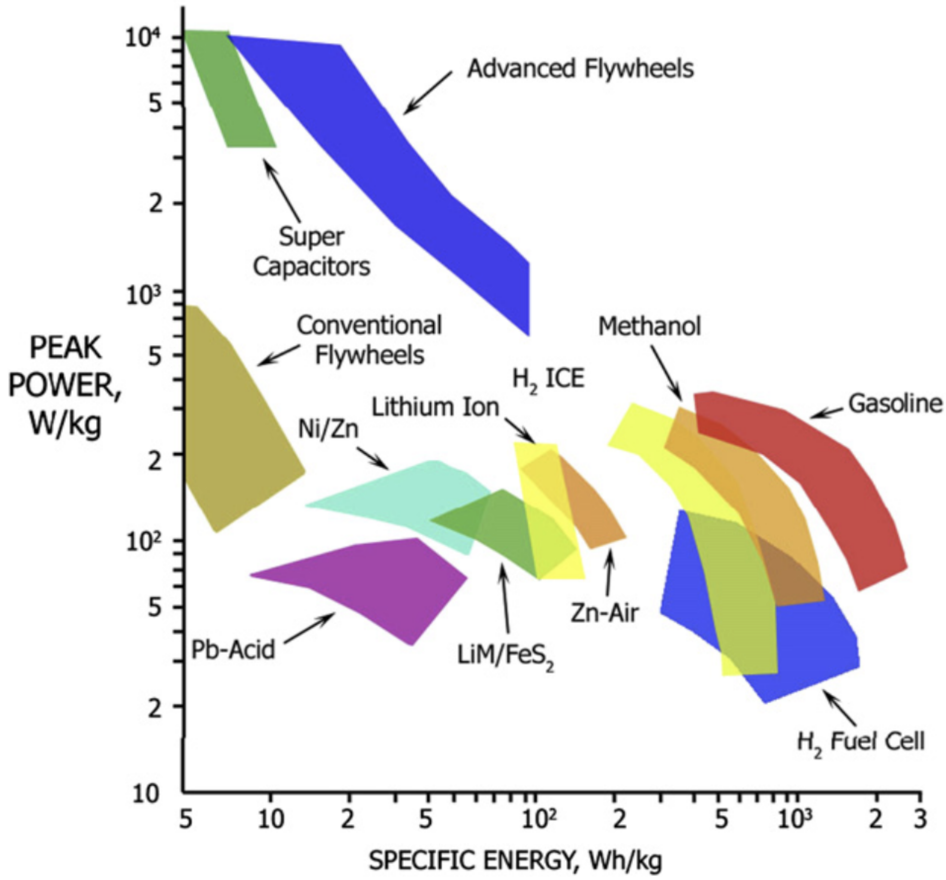

Figure 1.2: Ragone plot. Comparison of peak power versus energy storage capacity per mass [21].

A flywheel is a contraption which stores mechanical energy in a heavy and rapidly rotating mass. Flywheels have been used in industries for thousands of years such as in pottery and sewing, but the concept of large scale commercial energy storage applications for flywheels are relatively new and unexplored [9]. This raises an interest for exploring and investigating the function and possibilities of flywheels as a modern energy storage system.

1.2 Goal

The goal of this thesis is to research the design, function and applications of flywheel energy storage systems (FESS). This is achieved by a literature study where it is investigated how the different parts of a FESS works as well as the usage and applications of a FESS. A parameter study is also conducted to investigate how different parameters of a FESS affects its performance and function. The thesis also includes simulations of various scenarios where the different applications of FESS is demonstrated to understand how they perform under different circumstances.

1.3 Brief history of flywheels

The idea of storing mechanical energy in a rotating mass is not a new concept. Contraptions which uses the flywheel effect have been around for thousands of years. The first instance where flywheels were being used was as early as 6000 BC. At this time they were used as potter's wheels and hand held spindles [9]. At this time, the flywheels were human powered but preferable, as they could deliver a smoother experience than if the tools were powered directly by a human.

In the 18th century, in the industrial revolution, the flywheel gained new uses. Together with the newly emerged steam engines, the flywheel were used to turn the output power in to a smooth rotating motion [9]. Figure 1.3 shows a flywheel on a small single-cylinder steam engine train. These flywheels were made out of cast-iron.

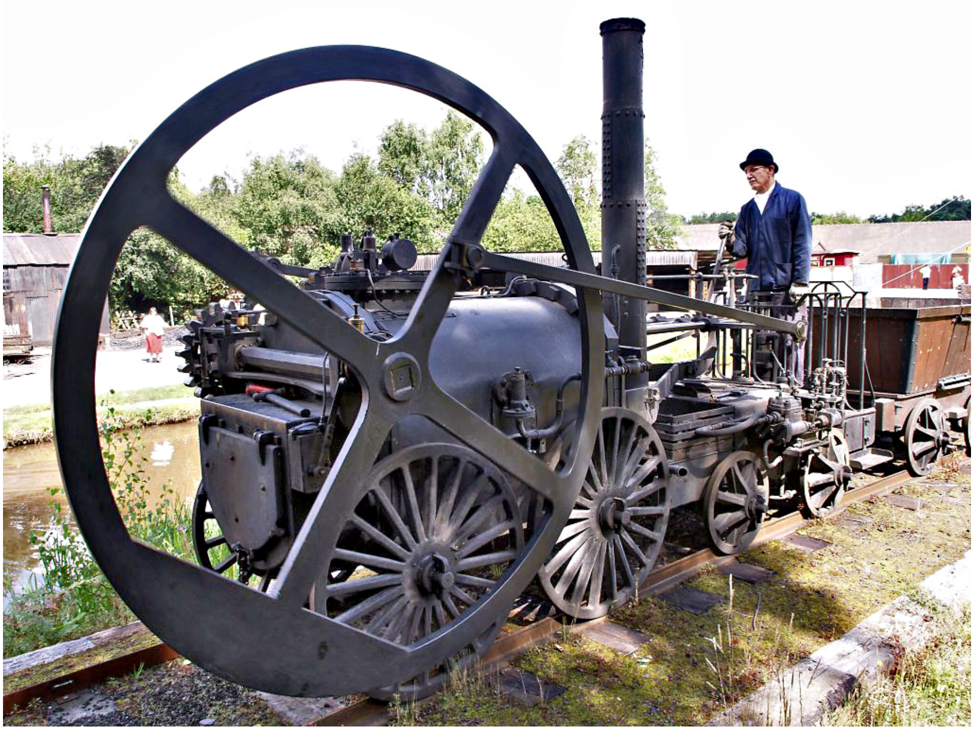

Figure 1.3: A flywheel being used to smooth the single-cylinder engine's output [57].

Older flywheels spun at much slower speeds than the modern flywheel and even though they weighed far more, the energy storing capacity was very low [9]. Failures with these flywheels were also common which could cause major destruction to the surroundings.

Flywheels as electric energy storage system was first proposed in the 1970's [11]. At this point in time, they were intended as a main energy storage system for electric vehicles. Their efficiency were still very low which did not make them ideal. In the 1980's, progress was made in both magnetic bearing and electric machines which increased the efficiency but electrochemical batteries were still superior in most applications. In the 1990's, a lot more research and investments were made to make the flywheel more efficient and sophisticated and paved the way for today's modern FESS [11].

1.4 Current projects

FESS is a relatively new technology and to this date there are only a few projects where flywheels are integrated in to the large-scale energy system. Beacon Power is a flywheel company and has two operating plants, one in New York and one in Pennsylvania, built in 2011 and 2014 respectively. Each plant has 20 MW installed capacity and provides frequency regulation for the nearby electrical grid. Figure 1.4 shows what the FESS plant in Stephentown, New York looks like. Beacon Power's flywheels can spin up to 16 000 RPM and is made to endure 175 000 charging cycles. Each plant consist of over 200 flywheels [41, 42].

Figure 1.4: Beacon Power's 20 MW plant in Stephentown, New York [42].

S4 Energy and ABB has built a hybrid battery and flywheel system to stabilize Netherlands' grid [2]. This plant has 9 MW installed capacity where 3 MW is from the flywheels and the rest from the electrochemical battery. The plant consists of six 5 000 kg flywheels which has a peak speed of 1 800 RPM. This plant also offers active support to the nearby Luna wind energy park. Figure 1.5 shows the flywheels in this plant.

Figure 1.5: ABB and S4's flywheels that stabilizes the Dutch grid [2].

Siemens Energy, together with the Australian grid operator ElectraNet, has implemented two flywheels to cope with grid instabilities in Robertstown, Australia [50]. As of late 2022, Siemens is also working on a 177 ton flywheel that is a part of a synchronous condenser [49]. This flywheel will work as a grid stabilization plant in Ireland.

2 Literature study

A FESS is a complex system combined of many parts. As figure 2.1 shows, a FESS includes a lot of different components which plays an essential role in the operation of a FESS. The main part of the FESS is the flywheel rotor itself, but parts as bearings, the electric machine, and the housing are also essential parts of the flywheel. In recent years the round-trip efficiency of FESSs are around 90-95 % [6]. The flywheel rotor can spin for up to a few days, but this varies on what type of rotor, the bearings used and how low of a vacuum there is in the housing.

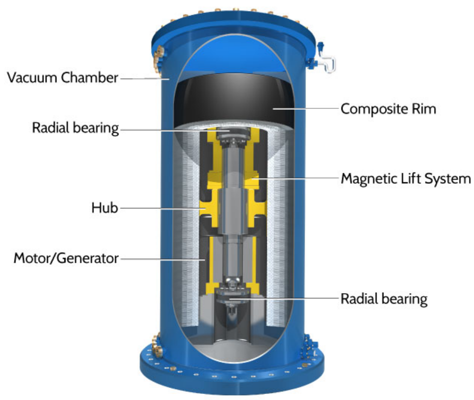

Figure 2.1: Illustration of a FESS [40].

2.1 Flywheel rotor

The flywheel rotor is where the mechanical energy is stored. There is usually two main classes of flywheels used when referring to they as an energy storage system. These are composite and steel rotors.

2.1.1 Composite flywheel

The composite flywheel is usually called the high speed flywheel and rotates at a speed typically in the 10^4-10^5 RPM range. The composite flywheel is usually assembled using materials such as carbon fiber, glass fiber, graphite or epoxy. These materials are what allows the flywheels to rotate at such high speed. This is because of the materials characteristics, being light as well as having high tensile strength allowance [32].

2.1.2 Steel flywheel

There hasn't been a lot of new research on the steel flywheels because of their reputation being 'older' technology and made for low speed flywheels. Although recently, the steel flywheels has regained some of its interest because of its low cost, better recyclability, and easy manufacturing. Some newer and higher performing steel flywheels has, despite its reputation, been getting some new recognition lately [32].

Table 2.1: Material characteristics for commercial fibers with K factor equal to 0.5. [33, 38].

Material	ρ [kg/m^3]	σ [GPa]	e_v [MJ/m^3]	e_m [kJ/kg]
Maraging steel	8000	2.7	1350	47
E-glass	2540	3.5	1750	190
S-glass	2520	4.8	2400	265
Kevlar	1450	3.8	1900	370
Spectra 1000	970	3.0	1500	430
T-700 graphite	1780	7.0	3500	545

Table 2.1 compares commonly used materials in commercial FESSs. ρ is the density of the material and σ is the maximum tensile strength. The energy density, e_v, and the specific energy, e_m, is calculated from equation 4.5 and 4.6 respectively.

2.1.3 Rotor shape

The rotor of a FESS can be several different shapes. As seen in equation 4.6 and 4.5 a shape factor, K, is introduced to accommodate for the geometries of the rotor. In figure 2.2, popular used shapes of the flywheel rotor are shown. The shape factor can be described as a measurement of the flywheel's material utilization. A laval disk for example has a K equal to 1 while a thin rim shape has a K approximately equal to 0.5. This means that the laval disk, also called equal stress disk, is a shape that maximises the mass to energy ratio [48].

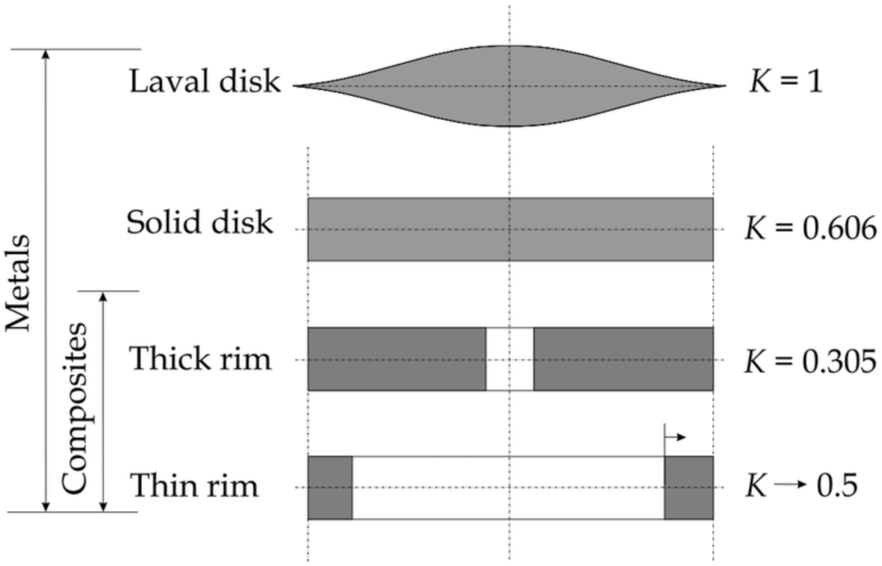

Figure 2.2: Different shapes for flywheel rotors [39].

2.2 Electric Machine

In FESSs the electric machine is essential. The electric machine acts as both a generator and a motor. When operating as a motor the electric machine converts supplied electric energy into mechanical energy by spinning the flywheel. When acting as a generator the electric machine slows down the flywheel, and turns the mechanical energy stored in the spinning flywheel into electric energy. The three main types of electric machines often used in FESSs are permanent magnet synchronous machine (PMSM), induction machine (IM) and variable reluctant machine (VRM). It is possible to use other types of electric machines in the FESS than those presented is this section.

2.2.1 Permanent magnet synchronous machine (PMSM)

A PMSM has high power density and efficiency and is a popular choice in FESS. The standard PMSM is typically the costliest machine out of the three presented. In return, it does not require a lot of maintenance. It's efficiency typically exceeds 90 % due to its low rotor losses. The PMSM is less rugged, and is more susceptible to temperature than the IM and VRM. Because the PMSM uses permanent magnets, demagnetization and idling losses are inevitable [32].

2.2.2 Induction machine (IM)

An IM is a very rugged machine, it has high torque and low cost. It is often used in high power applications due to these characteristics. The IM has some speed limitations, high maintenance and requires a complex control system. Due to these problems, as well as the IM's low efficiency, the PMSM is often the preferred machine to use in FESSs [6, 32].

2.2.3 Variable reluctant machine (VRM)

A VRM is a very robust machine and can be used in a wide range of speeds. It can operate in temperatures has high as 400 ℃ [20]. It often has better efficiency and easier controls when compared to the standard IM, when used under higher speeds. The VRM has lower power density and a low power factor compared to the PMSG. The VRM is considered to be a less mature machine than the PMSG and has not yet proved any potential to be better [20, 6].

2.3 Bearings

The bearings is a crucial part of the FESS. The design of bearings could reduce potential losses greatly as well as reducing maintenance requirements. The bearings should be designed to withstand the high rotation speeds of the flywheel while simultaneously providing a stable platform for its operation. The bearing system can either be mechanical or magnetic. Preferred system depends on weight, life cycle and loss importance.

(a) Mechanical bearing [26]. *(b) Magnetic bearings [7].*

Figure 2.3: Two types of bearings.

2.3.1 Mechanical bearings

Flywheels can use rolling elements bearings such as either ball bearings or roller bearing. Roller bearings often have higher radial load capacity than the ball bearings. However, ball bearings have higher capacity and lower friction during axial loads. When using mechanical bearings, a lubricant is needed. This lubricant will wear out and maintenance is needed. A FESS using mechanical bearings will usually dissipate half of its energy within a few hours due to different frictional losses [8].

2.3.2 Magnetic bearings

Magnetic bearings uses magnetic suspension to keep the axle stable. This means there aren't any contact between the axle and the bearings, thus the friction is close to zero. Because of the almost friction free environment the maintenance of the magnetic bearings is minimal and its lifetime almost indefinitely long. Magnetic bearings support the highest speed of any other bearings. There are both passive and active magnetic bearings [32]. Passive bearings uses permanent magnets to establish the magnetic suspension and are therefore inherently unstable. These will therefore almost never be used as the only bearing type, because the lack of control. Active magnetic bearings uses coils and can therefore vary the magnetic field to counteract any unwanted movement of the axle [20].

2.3.3 Hybrid bearings

Mechanical bearings are rarely used solely to support a flywheel, especially in high speed FESS. Instead a hybrid bearing system, using mechanical bearings in addition to magnetic bearings is often used. Another hybrid bearing system used is the combination of active and passive magnetic bearings. Both these types of hybrid bearings are widely used in FESS [32].

2.4 Housing

The housing primarily has two purposes. The first one is to maintain low pressure inside the housing such that the air drag becomes as low as possible. Secondly, it is a safety containment in case of a possible rotor failure. Often a vacuum pump is used to ensure as low pressure as possible in the housing. This pump does not need to operate frequently because of the absence of rotary seals due to the usage of electric machines [6]. The housing is usually made out of a thick layer of steel or other high strength materials. A sufficient cooling system is also necessary to remove the heat generated during operation. This is especially necessary in high speed FESSs because of the use of a vacuum pump. This is because of heat transfer is less effective in a vacuum rather than air [37]. Rather than using an expensive vacuum pump and cooling system, another approach is presented in reference [4]. Here a 50-50 mixture of air and helium is used. They claim that the windage loss can be reduced by 42 % of that in a 100 % air case. This is because of helium's gas density being approximately seven times less than air [4].

2.5 Safety

Due to the high mechanical energy stored in FESS, a small disturbance can cause major destruction. Installation of flywheels needs to be done in a way that does not set of a destructive chain reaction if one flywheel fails. Steel rotors typically bursts into three large chunks [43]. For composite rotors it was initially believed that they gradually broke into small debris and dust. An explosive failure became known to the industry, but not much information was published on this matter [43]. In 1995, an intentional failure during a test killed one of the test operators. The FESS tested stored under 1 kWh, but the test chamber lid was not bolted onto the chamber itself and ejected rotor material flew out with high speeds [10].

Beacon Power's plant, shown in figure 1.4, had a failure two weeks after its launch in July 2011. As seen in figure 2.4 one of the concrete covers were partially blown off. Beacon power responded to the accident by saying the flywheel failed the way it was supposed to fail and grinded itself into dust. Beacon Power Communication Director said that the cover came off due to safety features detected a rise in temperature and released water into the unit. This created steam which caused the pressure to increase to a level that blew off the concrete cover. All the dust that were spewed out of the flywheel containment were harmless carbon fiber dust [19].

Figure 2.4: Failure at Beacon Power's plant in 2011 [19].

In 2014, a suspension system in a steel based FESS experienced a failure and the rotor continued to spin 'like a top' until friction caused the rotor to burst because of the annealing taking place [10]. In 2015, a 100 kWh steel flywheel rotor was installed under a building. It then exploded some time after installation sending four people to the hospital [10]. The company, Quantum Energy Storage, was fined $58,025 for 16 health and safety violations. The flywheel rotor had come loose from its mooring and started to pulverize everything in its way [1].

There is no officially adopted standards in place for FESS safety as of today. Underground bunker containment is a possible solution such that the surrounding earth will absorb the forces from the burst. Another possible solution could be to make the rotor a stack of thinner discs. This would make the rotor release a fraction of the energy contained in it as the discs would be pulverized easier [6].

2.6 Cost

An important factor for FESS cost is the lack of large-scale manufacturing. In reference [43], it is suggested that the cost of a FESS can be split into two almost independent elements. The first being the flywheel rotor, bearings, housing, and ancillaries such as the vacuum pump (FW). The second cost is the motor/generator with power electronics, including a grid tied inverter (MGPE). The author, Keith R. Pullen, suggests that the cost for any given flywheel is given by:

$$COST(\$) = EC_{fw} + PC_{mgpe} \tag{2.1}$$

where C_{fw} $[\$/kWh]$ is the specific cost of the FW, C_{mgpe} $[\$/kW]$ is the cost of the MGPE, E is the capacity in kWh and P is the power in kW.

The author in [43] focuses on the steel based FESS and estimates C_{fw} to be around $800-1000 per kWh while the C_{mgpe} can be estimated from the cost of electric machines and inverters already in mass production today. The cost of the MGPE is estimated to be around $50-100 per kW. Since the power rating of the flywheel is much higher than the capacity (the ratio can exceed 100:1), it is the cost of the MGPE that dominates the total cost of the FESS. The composite based FESS does not have a lot of sources when it comes to the cost of it. But it is safe to assume that the C_{fw} would increase because the materials used in the rotor is more expensive. The bearings needed and the better performing vacuum pump would also increase the the cost of the FESS. In regards of the C_{mgpe}, it will also most likely increase as more expensive materials will need to be used as well as laminations need to be thinner [43, 47]. To this date FESSs are usually a lot more expensive than for example a lithium ion battery when capacity per dollar is being compared. For example, Beacon Power's FESS cost almost ten times more than what a similar capacity lithium ion battery plant would have been [32].

3 Applications

Due to the FESS's characteristics it has a lot of potential appliances. The FESS's low charge and discharge time makes it a good applicant to systems that experiences frequent changes. FESS's long life span and relatively low maintenance has also increased its popularity in different sectors.

3.1 Renewable energy integration

The global energy mix is becoming more and more complex with further integration of renewable energy. The increasing penetration of renewable energy sources, especially wind and solar, produces intermittent energy. Because of the FESS characteristics, it is a suitable option to store the energy produced from these intermittent energy sources. A FESS can adjust wind oscillations, improving the overall frequency [48]. There are considerable advantages to using FESSs as a backup for solar photovoltaic (PV). To promote the adoption of renewable energy systems, several FESSs have been developed, such as ABB's PowerStore, Urenco Power, Beacon Power, and VYCON technology for wind and solar applications. In 2010, the first high penetration solar PV and diesel power stations were installed in Western Australia, which supplied energy to Nullagine and Marble Bar. A FESS works as a UPS system, allowing maximum solar power injection during the day and ramping up diesel generators when the sun is not visible. This strategy results in a savings of 405,000 liters of fuel and a reduction of 1100 metric tons of greenhouse gas emissions annually. Furthermore, incorporating flywheels into the system has enabled the PV system to provide 60 % of the average daytime energy for both towns, generating 1 GWh of renewable energy per year [6].

3.2 Peak shaving

The energy demand for both households and industries follows trends. Energy companies can match and supply these trends when the energy source is an easily controllable energy source such as hydro power or fossil fuels. But with variable energy sources such as wind and solar power, the fastest growing energy sources in the world, it is harder to control the power output [44]. It can also be the other way around, where the electricity price can change as often as every hour, and the users lowers their consumption thereafter. The resulting energy overflow can then be stored by a FESS or equating energy storage systems.

As figure 3.1 illustrates, an energy storage system can store energy when the production is high and unload energy into the grid when production is low. This results in the power peaks on the grid becoming lower. As energy demand increases it is important to reduce the peaks so that the power cables does not need upgrading. Upgrading the power cables requires a lot of planning, manpower and money [51].

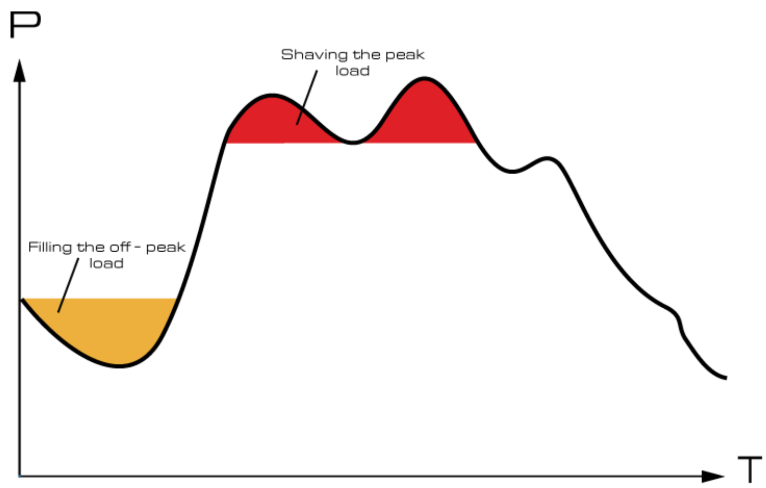

Figure 3.1: Illustration of peak shaving. P: Produced power, T: Time [51].

FESS can be used to reduce peaks on the grid by drawing power through activating the motor and increasing the rotational speed of the rotor when the peaks are high, essentially behaving as a load on the grid. To fill in the off-peaks the on the grid the flywheels electric machine operates in generator mode and converts the rotational energy stored in the FESS into electric power, behaving as a power source connected to the grid. Due to a FESS rapid charge and discharge time it can react quickly and shave unexpected peaks [6, 8].

3.3 Grid frequency balancing

Europe, Africa and most parts of Asia use AC currents with 50 Hz frequency. The countries that does not use 50 Hz use 60 Hz. Regardless of what frequency the power grid is using, the frequency is strictly regulated. Small deviations from the set frequency, even for a very short time, can damage equipment. These fluctuations in frequency occurs as a result of a difference in power supply and demand. When the grid is supplied with more power than what is demanded, the frequency increases as a result of the generators speeding up. In the other scenario, the frequency decreases when the demand is superior to the supply. These frequency fluctuations happens at a very high rate (almost every second) and the flywheels charge-discharge capabilities works really well with solving this problem [52].

The frequency is usually held within ±200 mHz of the nominal value in large networks. When the frequency exceeds a certain threshold, which can vary from grid to grid, a blackout is eminent. This is to prevent all of the equipment connected to the grid to not get damaged or destroyed. To avoid this happening, different measures are in place. If the frequency increases, the power plant production gradually decreases. Since most power plants takes a few minutes to react, energy storage systems have been used to draw some of the output power . In the same way, when the frequency decreases, gas reactors have historically been the most used option to supply power back to the grid [52].

FESS can be used to regulate frequency deviations by either supplying the grid with power if the load is lower than the production, or draw power if the load is higher than the production. The quick charge and discharge time of a FESS makes it suitable for frequency regulation as the power that is fed into, or taking out of, the grid can vary almost instantly [32].

3.4 Voltage sag control

Power faults or unbalance in the grid can result in the voltage magnitude to decrease. For sensitive loads, such as semiconductor manufacturing, paper making and high frequency power electronics, voltage sag has become a major problem [6]. 92 % of power quality problems are a result from voltage sag and 80 % of these problems only last for for 20-50 ms [59].

In reference [58], a 10 MJ FESS is presented. This system was set up and tested in the year 2000. The FESS was implemented in a distribution network to keep a power quality high and have a reliable power supply. The FESS was able to keep the voltage magnitude within 98-102 % of its nominal value. The system could supply 10 kW of power for 15 minutes.

3.5 Uninterruptible power supply (UPS)

An uninterruptible power supply (UPS) is a short term energy storage with control electronics. One of the most successful application for the flywheel is as an UPS. More than 80 % of all power disturbances last for less than a second, and 97 % of them last for less than 3 seconds [24, 48]. These power disturbances causes voltage and frequency problems, as well a regular power interruptions. As of now the most widely used UPS is electrochemical batteries. For those power outages which are in the longer timespan, ≥15 seconds, electrochemical batteries are a good UPS because of their high energy density. While for power outages shorter than 15 seconds the FESSs short discharge and charge time, as well as its lifetime independence of the depth of discharge, are great properties. The combination of batteries and FESSs is a good UPS system for solving most of the power outage problems. The combination of the energy storage methods could increase the batteries life time, because charge and discharge frequency would not be as high as it otherwise would have been without a FESS.

Quite a few manufactures are already using FESSs as a UPS. VYCON's VDC has a max power rating of 450 kW and a max energy storage of 1.7 kWh [56]. Electricity de Acores is a Portuguese power company which installed a power system on the Portuguese island, Flores. The power system is consisting of wind turbines, hydro generators, diesel generators and a FESS with a 500 kW power rating and a capacity of 5 kWh [23]. One of the earliest FESS UPS was in München, Germany as early as 1973. It was rated for 155 MW [6].

3.6 Other applications

FESSs is not only used for large scale power applications, but also in transportation, motorsports and space.

3.6.1 Transportation

The flywheel has been used for a long time in cars and vehicles to smooth out the power pulses coming from the engine. Due to most engines being a four stroke engine, where only one of these strokes is the power stroke, the flywheel helps balancing the power output of the engine. The FESS has also been proposed to use in light trail transits. A study, reference [46], found a result of 31 % energy savings using a 725 kW flywheel with a capacity of 2.9 kWh in a light trail transit in Alberta, Canada.

3.6.2 Motorsports

FESSs has been used in motorsports in a few cases. Small and compact FESSs are used in hybrid systems to store breaking power and deliver instant torque with the electric motors when the car accelerates. The FESSs used in automotives usually only stores a few hundred watt hours and can deliver around a hundred kilowatts of power [25]. Because they store very little energy, an electrochemical battery is usually preferred in transportation but in motorsports a small FESS which can supply small bursts of high power can be favoured [54].

3.6.3 Space

In devices orbiting the earth, FESSs can provide both energy storage and attitude control. The NASA Glenn Research Centre has for the past decade been interested in developing a FESS for space vehicles. The proposed system has a peak power of 4.1 kW and capable of storing 15 MJ. It is a composite rotor and has magnetic bearings, with an efficiency of 93.7 %. NASA has made some estimates on replacing space station batteries with this flywheel system and the estimates result in savings upwards of $200 million [34].

4 Theory

4.1 Flywheel rotor

The moment of inertia is calculated by the integral shown below in equation 4.1.

$$I = \int r^2 \, dm \tag{4.1}$$

r is the radius of the object and m is the mass. Performing this integral for a solid cylinder yields equation 4.2. Integrating over a hollow cylinder gives equation 4.3. r_1 is the inner radius of the hollow cylinder and r_2 is the outer most radius.

$$I = \frac{1}{2}m \cdot r^2 \tag{4.2}$$

$$I = \frac{1}{2}m(r_1^2 + r_2^2) \tag{4.3}$$

The kinetic energy stored in the rotating flywheel is given by equation 4.4.

$$E = \frac{1}{2} \cdot I \cdot \omega^2 \tag{4.4}$$

E is the stored kinetic energy, I is the moment of inertia, and ω is the angular velocity.

Equation 4.6 and 4.5 shows the maximum kinetic energy able to be stored in the rotor per unit volume and mass respectively.

$$e_v = K \cdot \sigma \tag{4.5}$$

$$e_m = K \cdot \frac{\sigma}{\rho} \tag{4.6}$$

K is the shape factor, ρ is the mass density and σ the maximum tensile strength.

4.1.1 Flywheel model

A mechanical torque balance of the FESS is displayed by equation 4.7. In this equation, the total torque of the system equals the torque in and out of the FESS's rotor minus the torque lost from friction and air resistance. When the FESS charges, $\tau_{in/out}$ is positive and when it discharges, it is negative. The torque lost in the FESS, τ_{losses}, can be assumed a function of the angular velocity multiplied by a friction value, R. The systems total torque can be substituted by the change of angular momentum as shown in equation 4.8.

$$\sum \tau_{sys} = \tau_{in/out} - \tau_{losses} \tag{4.7}$$

$$\sum \tau = \frac{d}{dt}L \tag{4.8}$$

This results in equation 4.9. This differential equation is a model of the FESS where the change in rotational momentum is a function of torque in/out minus the losses.

$$\frac{d}{dt}L = \tau_{in/out} - R\omega \tag{4.9}$$

The relationship between the angular momentum, sometimes called spin, and the angular velocity is given by equation 4.10. Substituting this into equation 4.9 results in equation 4.11 which is an easier to understand differential equation where the change in rotational speed is equal to the torque in/out minus the losses all divided by the moment of inertia.

$$L = I\omega \Leftrightarrow \omega = \frac{L}{I} \tag{4.10}$$

$$\frac{d}{dt}\omega = \frac{\tau_{in/out} - R\omega}{I} \tag{4.11}$$

Substituting equation 4.10 into equation 4.4 yields equation 4.12 where the rotational kinetic energy stored in the FESS is a function of the angular momentum.

$$E = \frac{1}{2} \cdot \frac{L^2}{I} \tag{4.12}$$

4.1.2 Rotor losses

The mechanical resistance, R, in the flywheel model is a function that includes losses from air drag, friction, hysteresis and eddy-currents [29]. Equation 4.13 models the resistance in the FESS as a function of the rotational velocity.

$$R(\omega) = A\omega^2 + B\omega + C \tag{4.13}$$

The coefficients A, B and C is the air drag, eddy-current and hysteresis coefficient, respectively [29]. The air drag is the friction between the rotor surface and the air molecules. The eddy-currents in the FESS is the swirling of fluids around the rotor creating reverse currents of air. The hysteresis is internal friction within the rotors material.

4.2 Electric machines

An electric machine is a device that transforms electric energy to mechanical energy or vice versa with electromagnetic forces. Hence an electric machine can function both as an electric motor and a generator [17].

The mechanical power an electrical motor can deliver to the rotor is given by equation 4.14. The power to the rotor is proportional to the electrical power that the machine draws from the grid multiplied by the efficiency of the machine in motoring mode. The efficiency of an electric motor is usually very high due to the losses being very small. The losses in the machine include mechanical friction, electromagnetically losses in the air gap, electrical losses in the windings.

$$P_{mech} = \tau \cdot \omega = P_{el} \cdot \eta_{motor} \tag{4.14}$$

Similarly, for an electric machine operating in generator mode, the electric power converted from mechanical power is given by equation 4.15. A generator will also have a very high efficiency.

$$P_{el} = P_{mech} \cdot \eta_{generator} = \tau \cdot \omega \cdot \eta_{generator} \tag{4.15}$$

4.2.1 Permanent magnet synchronous machine (PMSM)

The synchronous machine is a machine where the rotor rotates as fast as the induced magnetic field in the armature windings [15]. The formula for the synchronous rotational speed, n_s, in RPM is shown in equation 4.16, where f is the frequency of the current feeding the armature windings and $Poles$ is the number of magnetic poles in the machine [30]. Because the synchronous speed is a function of the frequency of the current, a FESS will have to use a frequency converter to change the speeds of the machine [45].

$$n_s = \frac{f \cdot 120}{Poles} \tag{4.16}$$

A PMSM is a type of synchronous machine that uses permanent magnets in stead of letting a current induce a magnetic field in the rotor. The torque-speed characteristics of a PMSM has two modes [14]. As figure 4.1 shows, the PMSM is in a constant torque mode from standstill to the nominal speed, ω_{rated}. In this mode the torque delivered to the load is constant meaning the power is a function of the rotational velocity as seen in equation 4.17 and the power is proportional to the rotational speed.

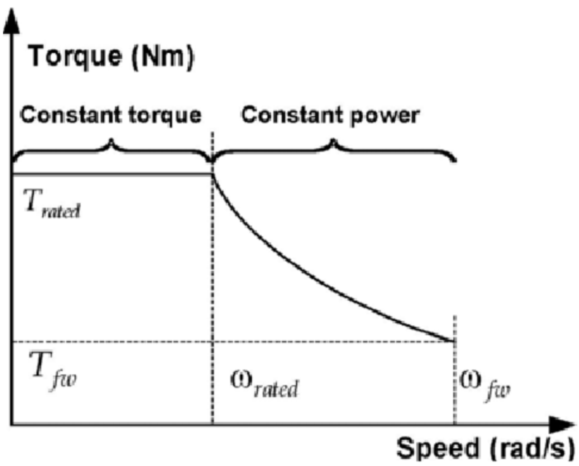

Figure 4.1: Torque-speed characteristics for a PMSM [14].

$$P(\omega) = \tau_{rated} \cdot \omega \tag{4.17}$$

From the nominal speed and above, the PMSM is in the constant power mode. In this mode the power delivered to the load is constant while the torque is a function of the rotational velocity as seen in equation 4.18. Because the power is constant in this mode, the torque is inverse proportional to the rotational speed.

$$\tau(\omega) = \frac{P_{max}}{\omega} \tag{4.18}$$

4.2.2 Induction machine (IM)

The IM (or asynchronous machine) is an electric machine where the rotor rotates either slower or faster than the magnetic fields in the stator [30]. The difference between the rotor and the stator speeds is called slip and is due to the geometry of the stator windings. The formula for slip is given by equation 4.19 where s is the slip, n is the rotational speed of the machine and n_s is the synchronous speed.

$$s = 1 - \frac{n}{n_s} \tag{4.19}$$

As figure 4.2 shows, the torque from an IM is dependent on the slip. When the slip is between zero and one, the machine functions as a motor and when the slip is less than zero, the machine is in generator mode. There is also optimal slip values for both motoring mode and generating mode where the torque is highest.

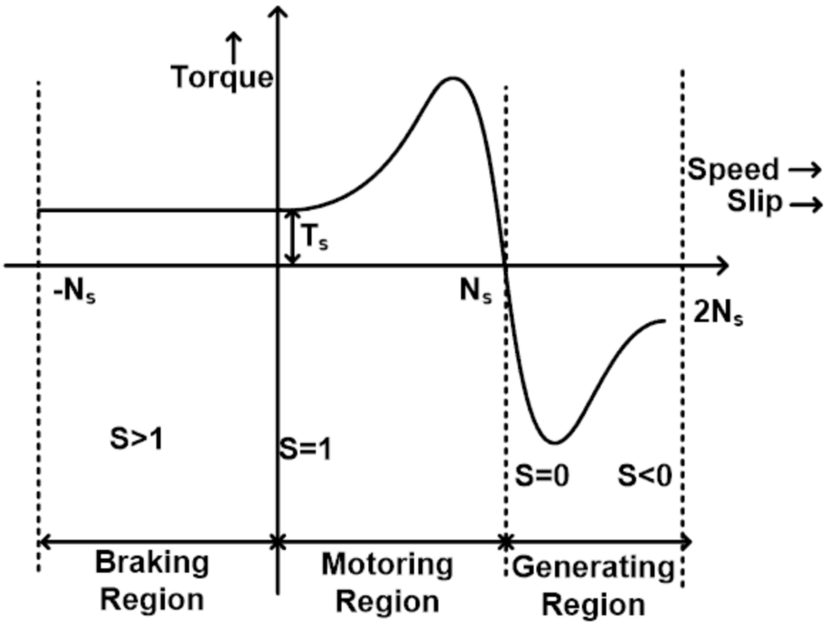

Figure 4.2: Torque-speed characteristics for an IM [53].

The torque from an induction machine is found with equation 4.20 where ω_s is the synchronous rotational velocity, V_{TH} is the equivalent circuit's Thevenin voltage, R_{TH} and X_{TH} is the Thevenin equivalent resistance and reactance and R_2' and X_2' is the transformed resistance and reactance from the secondary side [30].

$$\tau(s) = \frac{3V_{TH}^2 \cdot R_2'/s}{\omega_s((R_{TH} + R_2'/s)^2 + (X_{TH} + X_2')^2)} \tag{4.20}$$

4.2.3 Variable reluctance machine (VRM)

The VRM is a machine where the magnetic field in the rotor is dependent on its position relative to the poles on the stator. As the rotor rotates, the magnetic flux changes, which creates a varying reluctance that leads to torque generation [31].

The torque from a VRM consists of three modes. As figure 4.3 shows, the 2 first modes of the VRM are identical to the PMSM. In the third mode, the natural mode, the torque multiplied with the rotational velocity squared is constant. Equation 4.21 shows the resulting expression for the torque as a function of the rotational velocity where τ_{rated} is the torque at the constant torque mode, ω_{mb} is the rotational velocity where the machine changes from constant torque to constant power mode and ω_{mp} is the rotational velocity where the the machine changes from constant power to natural mode.

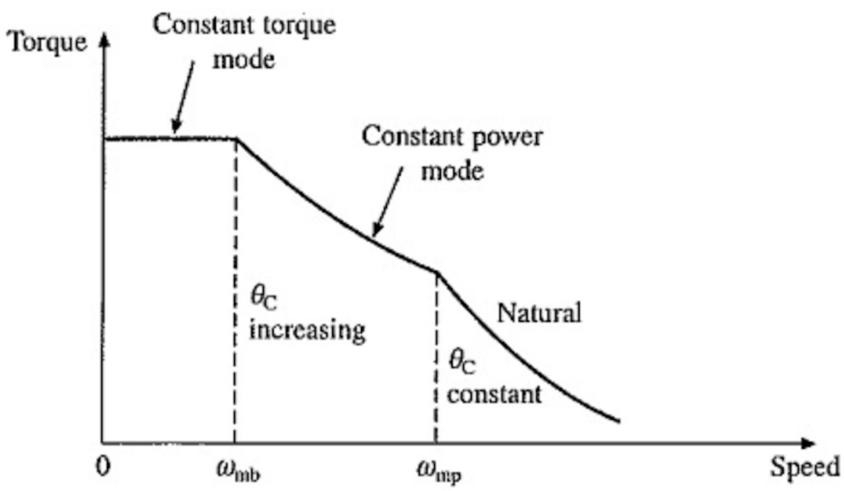

Figure 4.3: Torque-speed characteristics for a VRM [22].

$$\tau(\omega) = \frac{\tau_{rated} \cdot \omega_{mb} \cdot \omega_{mp}}{\omega^2} \tag{4.21}$$

4.3 Control system

In cases where a system needs to turn on and off quickly while responding fast, a controller is often used to minimize wear and tear on equipment. The proportional integral derivative (PID) controller is a popular controller that can be both very stable and fast if tuned right. In a FESS, the controller is used to control the electric machine in cases where it needs to react quickly, for example when used for frequency regulation [12]. The controller continuously compares the output of a system with the desired reference and adjusts the input control signal to minimize the error. The three parts of the PID controller is described here [12]:

Proportional (P) Control: The proportional term produces an output that is proportional to the current error, which is the difference between the desired reference and the actual output. The proportional gain determines how aggressively the controller responds to the error. Increasing the proportional gain makes the controller react more strongly to errors, but it can also lead to overshoots and instabilities in the system.

Integral (I) Control: The integral term takes into account the accumulated past errors over time. It integrates the error signal, which helps eliminate steady-state errors that cannot be corrected by proportional control alone. The integral gain determines how quickly the integral term accumulates and influences the response of the controller to sustained errors.

Derivative (D) Control: The derivative term considers the rate of change of the error. It anticipates the future behavior of the system based on the current rate of error change. The derivative term is useful for damping the response of the system and reducing overshoot and oscillations. The derivative gain determines the sensitivity of the controller to changes in the error rate.

The PID controller output is calculated as the sum of the proportional, K_p, integral, T_i, and derivative, T_d, components. The control signal is applied to the system, and the process repeats, continuously adjusting the control signal to keep the error minimized and maintain the desired reference value.

Laplace transforms is commonly used when tuning controllers. A Laplace transform is a mathematical transform which turns a function of a real variable into a function of the complex variable s [13]. This makes many differential equations easier to solve and allows for easier block diagram manipulations. Equation 4.22 shows how a function is Laplace transformed and equation 4.23 shows the Laplace transform for a PID controller in the product form, where n is usually set to 10 [12].

$$F(s) = \int_0^\infty f(t)e^{s\cdot t}\,dt \tag{4.22}$$

$$h_{PID}(s) = K_p \cdot \frac{1 + T_i \cdot s}{T_i \cdot s} \cdot \frac{1 + T_d \cdot s}{1 + \frac{T_d}{n} \cdot s} \tag{4.23}$$

Figure 4.4 shows an example of an open and closed feedback loop as block diagrams. Each block in the block diagram is often expressed as Laplace transformed transfer functions. To tune a PID controller, the open loop function *without* the controller, h_0^*, is investigated.

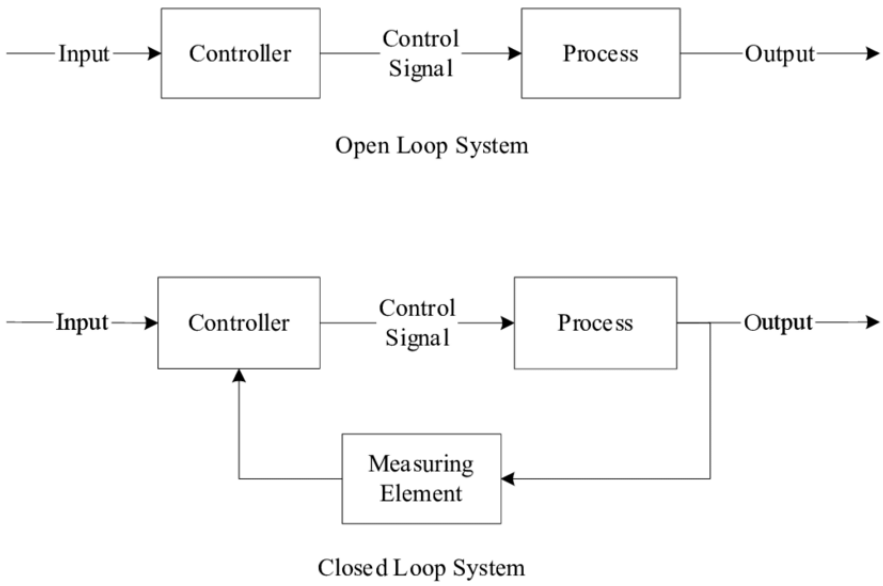

Figure 4.4: Example of an open and closed feedback loop [5].

The phase margin, Pm, is the difference in phase shift from -180 ° at the same frequency as the magnitude of the function is equal to zero. Similarly, the gain margin, Gm, is the negative magnitude at the same frequency as when the phase shift is equal to -180 ° [12].

Table 4.1: Gain and phase margin for different response types [12].

Response type	**Nr. of half periods**	**Gm [dB]**	**Pm [°]**
Minimum amplitude	10-15	4	15
Minimum area	4-6	8	30
Minimum disturbance	1-2	12	45

The bode plot of h_0^* is plotted and the frequency at which the phase is at (-200 ° - Pm) is obtained and the magnitude at this frequency is found. Equation 4.24 is a proposed method to find a suiting value for K_p and similarly equation 4.25 and equation 4.26 are proposed method to find suiting values for T_i and T_d [12].

$$K_p = \mid h_0^*(\omega_w) \mid_{dB} - 4 \; dB \tag{4.24}$$

$$T_i = \frac{2.8}{\omega_w} \tag{4.25}$$

$$T_d = \frac{1}{\omega_w} \tag{4.26}$$

The values found are put in to equation 4.23 and the margins of the open loop transfer function *with* the controller, h_0, is analysed. If the requirements for the gain and phase margins, from table 4.1, are met, the PID controller should be tuned properly. If not, the K_p needs to be decreased until the desired margins are met [12].

To simplify and reduce block diagrams there are many rules. Figure 4.5 shows two commonly used reduction rules. The uppermost reduction is the commutative property where two transfer functions consecutively can be multiplied together. The bottom rule is a reduction rule for negative feedback loops which is commonly used for control system loops [35].

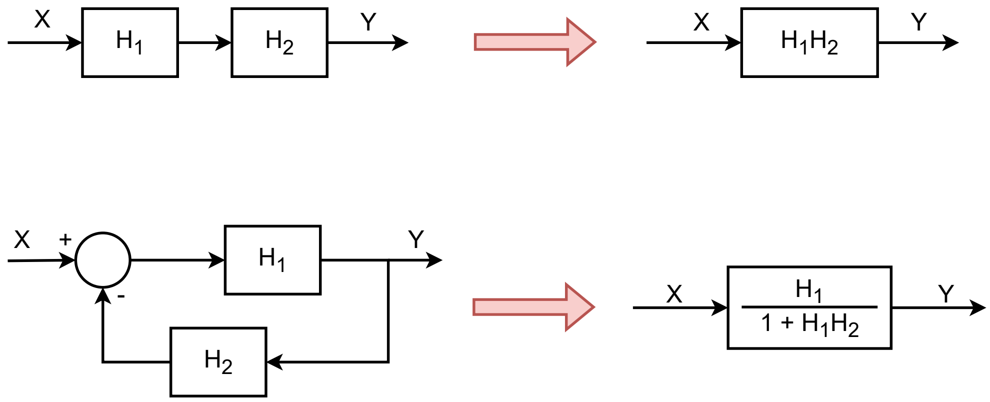

Figure 4.5: Reduction rules for commutative properties and negative feedback loop in block diagrams.

4.4 Electric grid

Connecting the FESS to a grid is done using power electronics. To make sure the current out of the FESS matches the frequency of the grid and the electric machines get the required frequency to spin at the desired speeds. The alternating current (AC) from the grid is transformed into direct current (DC) where a signal generator or a frequency converter is used to deliver a specific frequency and a thus a specific synchronous speed for the electric machine [16]. It is assumed, in this report, that this process is ideal without any power losses. It is also assumed that the grid and its cables is perfect conductors meaning it behaves non-resistive, non-inductive and without any power losses.

5 Results and discussion of simulations

Simulations are used to investigate and visualize FESS both isolated and in systems to showcase their applications. The dynamics of the FESS is simulated in MATLAB using equation 4.9 to calculate the spin. Equation 4.10 and equation 4.12 is then used to calculate the stored energy and rotor speed respectively. The results of the simulations will also be discussed in this section.

5.1 Parameter study

To study the different parameters in a FESS, a parameter study is conducted to compare and analyze how they affect the performance. Several simulations are performed where only one parameter of the flywheel is changed to be able to analyze the difference the parameters makes.

5.1.1 Different rotors

To see how different rotor shapes affect the flywheel, an arbitrary FESS is simulated with different rotors. The code for the simulations are attached in Appendix A. Table 5.1 shows the parameters for the simulation of rotors with different shapes. The shapes compared is a solid cylinder and hollow cylinders with a thin rim and one with a thick rim. It is assumed the flywheels are made out of the same material thus the same density. The length and outer radius are the same. All the flywheels are powered by the same PMSM that can supply a constant torque of 228 Nm within the nominal rotor speed of 9000 RPM, where the motor cuts off to not get damaged.

Table 5.1: Parameters for different rotor shapes where r_1 is inner radius and r_2 is outer radius.

Rotor shape	Radius [m]	Mass [kg]	Moment of inertia [kg m^2]
Solid cylinder	0.6	1300	234 (eq 4.2)
Thin rim	r_1 = 0.45, r_2=0.6	568.75	159.96 (eq 4.3)
Thick rim	r_1 = 0.3, r_2=0.6	975	219.38 (eq 4.3)

Figure 5.1 shows the energy stored in the FESS with different shapes while charging with maximum torque and figure 5.2 shows their corresponding rotor speeds. Only the charging is simulated as the discharging would be the exact same only inverted. This is because the PMSG is able to supply the same torque for charging and discharging and the mechanical losses in the rotor is negligible in the short time span of charging and discharging.

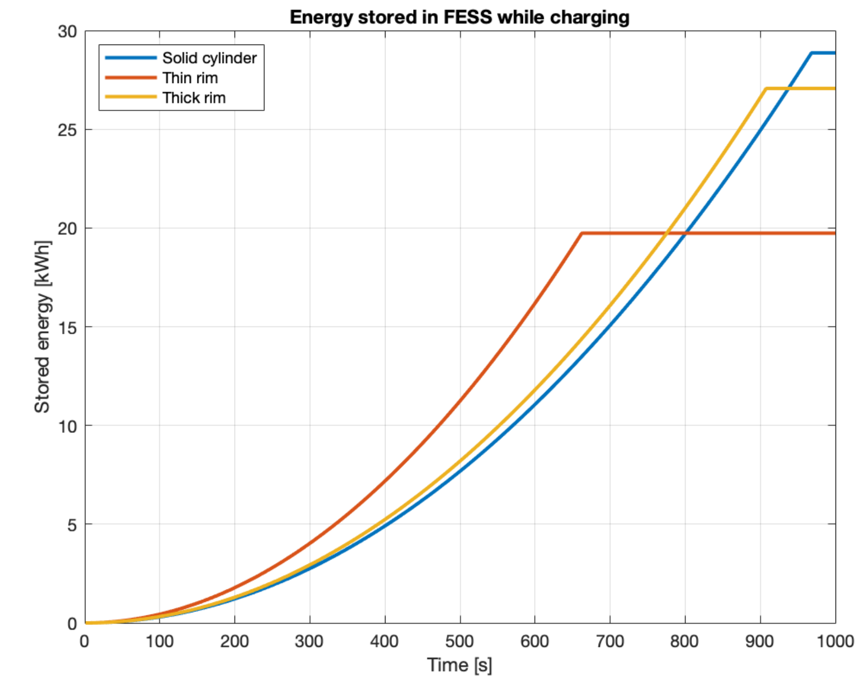

Figure 5.1: Energy stored while charging FESS with different rotor shapes.

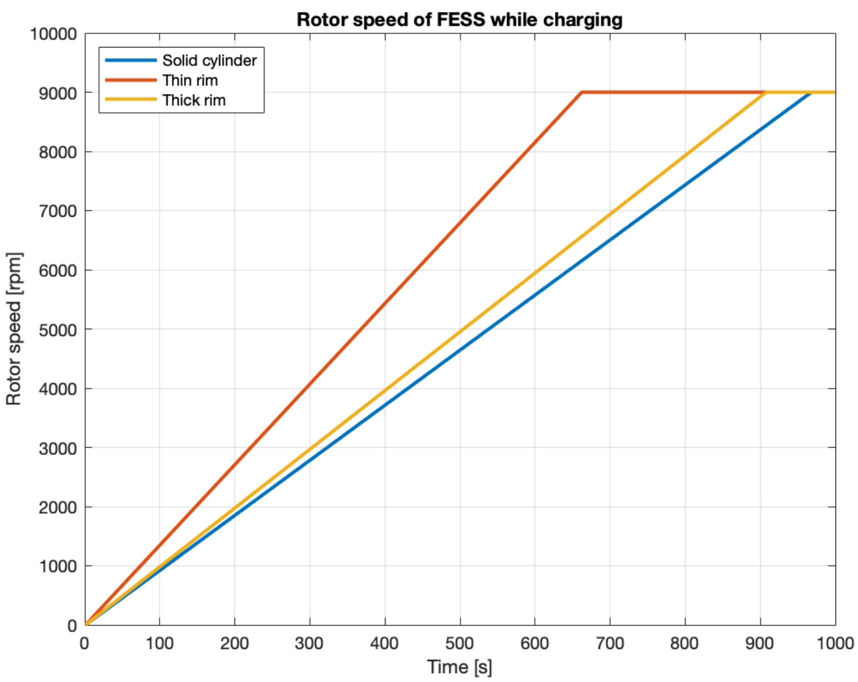

Figure 5.2: Rotor speed during charging of FESS with different rotor shapes.

It is observed that a thinner rim charges faster and due to the rotational speed increasing faster, the rotor reaches its nominal speed faster and the motor cuts off sooner. This means that the total amount stored in the FESS is lower for thinner rims. In applications where it requires a high power output but the amount of energy does not need to be very high, a thinner rim is more applicable.

Different rotor masses and rotor radii are simulated to analyze the difference it makes in a FESS. Table 5.2 shows the different rotors simulated. The electric machine used to charge and discharge the FESSs in this simulation is the same as for the different rotor shapes.

Table 5.2: Parameters for different rotor masses and radii. Moment of inertia calculated with equation 4.2

Rotor shape	Radius [m]	Mass [kg]	Moment of inertia [kg m^2]
Solid cylinder	0.6	1300	234
Solid cylinder	0.6	1600	288
Solid cylinder	0.9	1300	650
Solid cylinder	0.9	1600	800

Figure 5.3 shows the energy stored in the FESS with different masses and radii while charging. The rotational speed of the FESS is shown in figure 5.4.

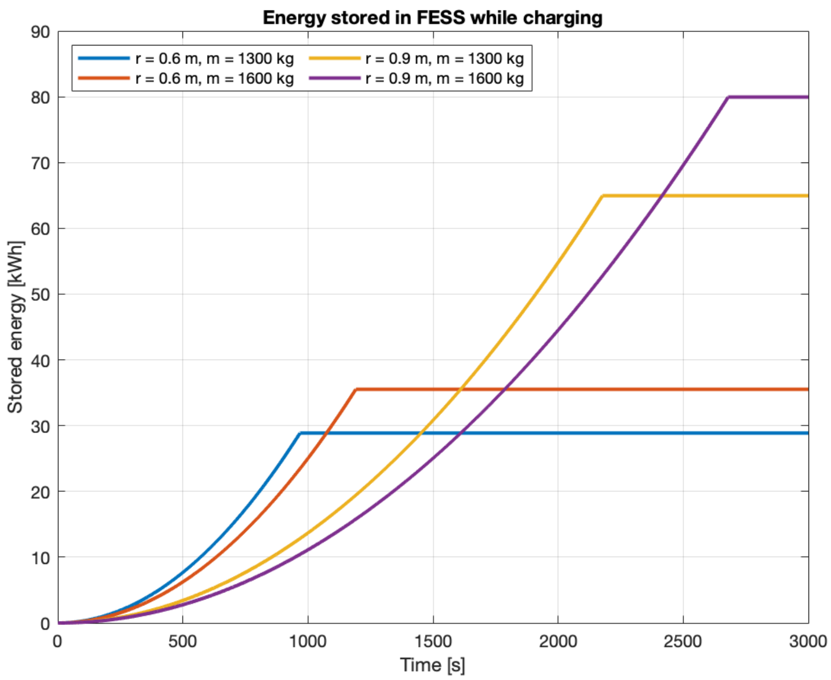

Figure 5.3: Energy stored while charging FESS with different rotor masses and radii.

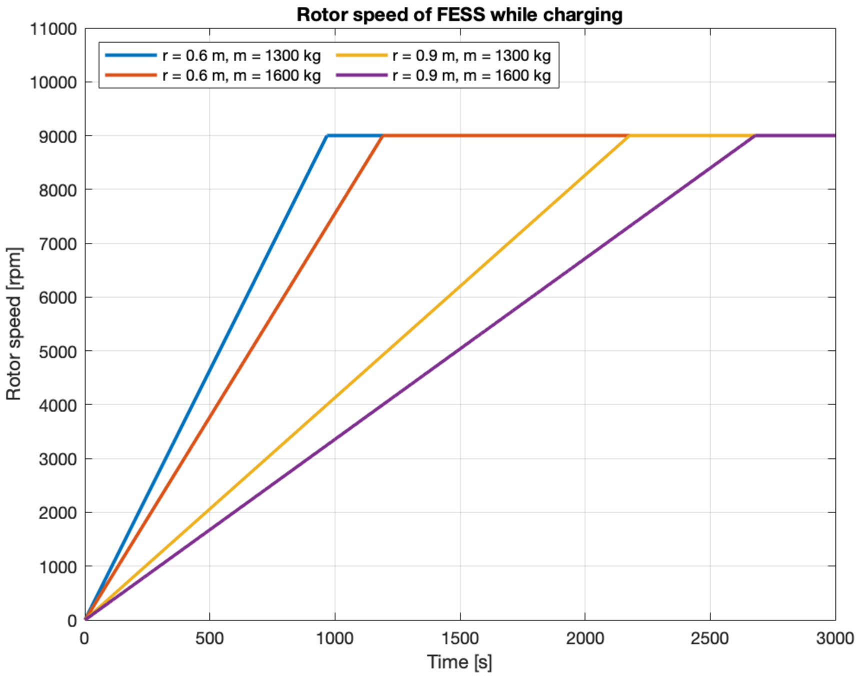

Figure 5.4: Rotational speed of FESS with different rotor masses and radii while charging.

From equation 4.2 it is observed the the moment of inertia for a solid cylinder is proportional to the mass and proportional to the radius squared. As equation 4.11 shows, the change in rotational velocity is inverse proportional to the moment of inertia. Therefore, it makes sense that the FESS with smaller radii charges faster, as seen in figure 5.4. As seen in equation 4.4, the energy stored in the FESS is proportional to the moment of inertia. Therefore, the total energy stored in the FESS at maximum rotational speeds is higher for FESS with higher moment of inertia.

It can be seen that increasing the radius will increase the energy capacity of the FESS more than increasing the mass. But if the desired property of the FESS is to charge and discharge fast, keeping a smaller radius might be ideal.

5.1.2 Different electrical machines

To see how the different types of electrical machines and their torque characteristics affect the charging and discharging of a FESS, a simulation is done with four different electrical machines. As table 5.3 shows, the machines simulated includes two PMSM with different nominal speeds and maximum torques, an IM and a VRM. The code for the simulations are attached in Appendix B where the parameters of the IM also are found.

Table 5.3: Types of electrical machines used.

Machine type	Speed characteristics [RPM]	Max torque [Nm]
PMSM (1)	$n_n = 9\ 000$	228
PMSM (2)	$n_n = 3\ 000$	300
IM	$n_s = 12\ 000$	292
VRM	$n_{mb} = 5\ 000$, $n_{mp} = 9\ 000$	280

The torque produced by the different electrical machines are displayed in figure 5.5 from stationary to the maximum rotational speed which is set at 12 000 RPM.

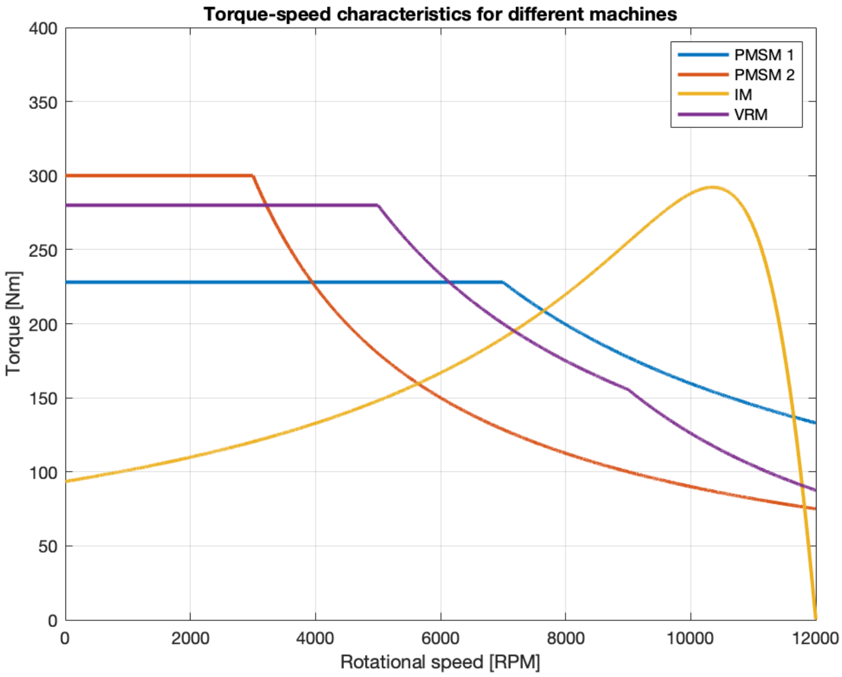

Figure 5.5: Torque-speed characteristics of different electrical machines.

Figure 5.6 shows energy stored in the FESS while charging with the different electrical machines.

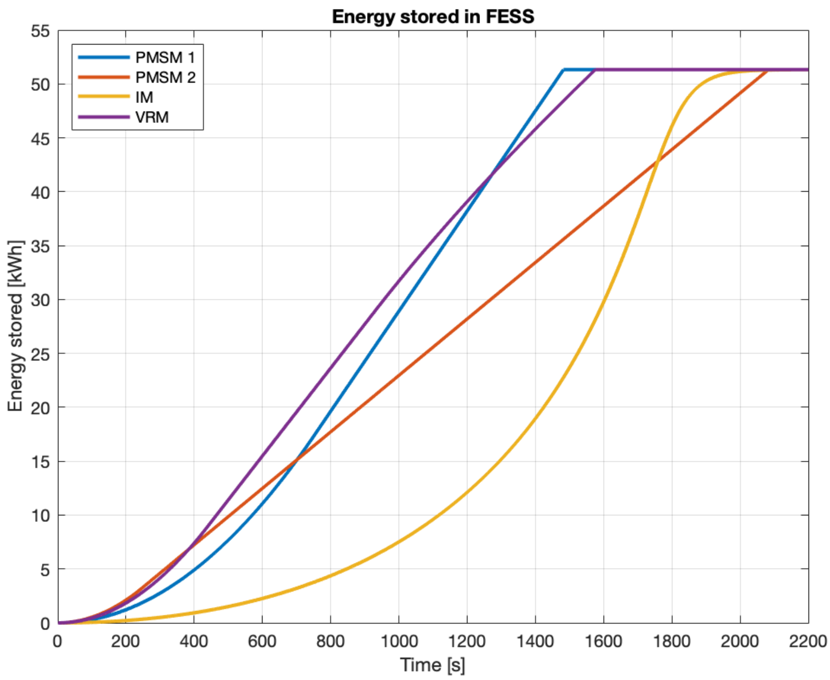

Figure 5.6: Energy stored in FESS while charging with different electrical machines.

For the two PMSMs and the VRM, a higher max torque charges the FESS quicker. As figure 5.6 shows, *PMSM 2* has a sudden bend where the charging rate reduces rapidly. This is due to the nominal speed being low and the maximum power being lower relative to the other machines. This means that if a PMSM or a VRM, is to be used in a high speed FESS, it needs a high nominal speed.

The IM charges slowly at low speeds and at very high speeds, but while operating in the range in between about 8 000 - 11 000 RPM, it charges quickly. And while the torque from the other electrical machines decreases at higher speeds the IM's torque increases (until a point where it decreases very rapidly as figure 5.5 shows). Usually, an IM would have a frequency converter to keep a constant, and optimal, slip after start up.

5.1.3 Spin out time and mechanical losses

To see how the FESS maintains its stored energy, simulations are done to study the spin out time for different losses with equation 4.13 by changing the parameters A, B and C. The modeled FESS has a solid cylinder rotor with a mass of 1300 kg and a radius of 0.6 m. The initial rotational speed is 10 000 RPM and the simulations are done over the period of a month. The code for the simulations are attached in Appendix C.

Figure 5.7 shows spin out time of the FESS with the resistance coefficient A, air drag coefficient, ranging from to $50 \cdot 10^{-12}$ to $10 \cdot 10^{-9}$ and the B and C coefficient equal to 0. As A increases, the spin out time decreases.

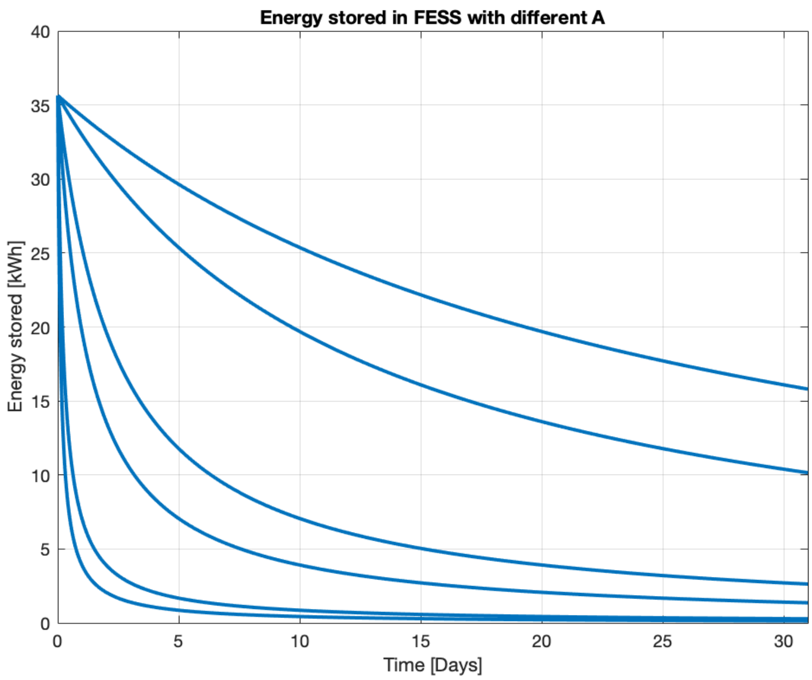

Figure 5.7: Spin out time of FESS with different resistance coefficient A.

Figure 5.8 shows the spin out time of the FESS with the resistance coefficient B, the eddy-current coefficient, ranging from $1 \cdot 10^{-6}$ to $50 \cdot 10^{-9}$ and the A and C coefficient equal to 0. Increasing B reduces the spin out time.

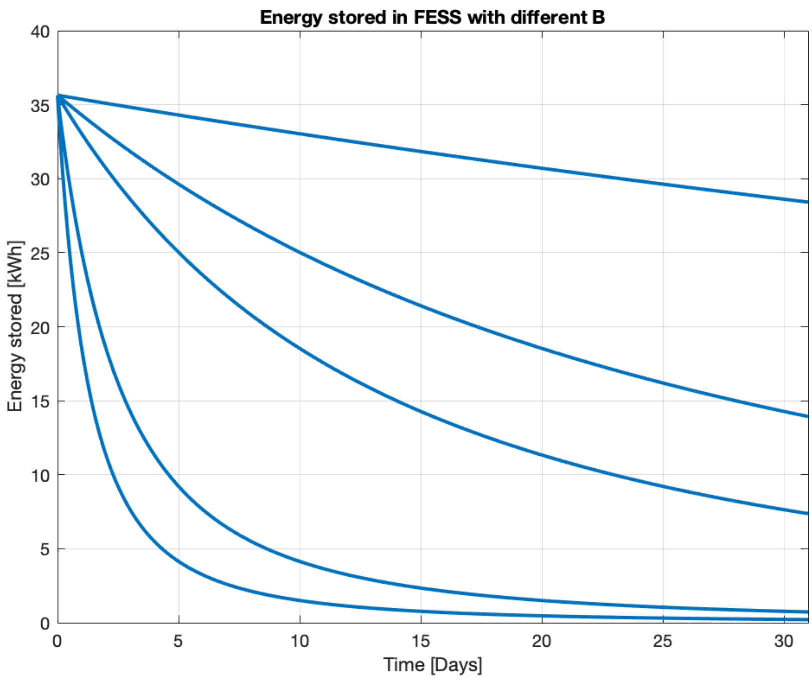

Figure 5.8: Spin out time of FESS with different resistance coefficient B.

Figure 5.9 shows the spin out time for the simulated FESS with the resistance coefficient C, the hysteresis coefficient, ranging from $50{\cdot}10^{-6}$ to $1{\cdot}10^{-3}$ and the A and B coefficients equal to 0. The higher C is, the faster the FESS discharges.

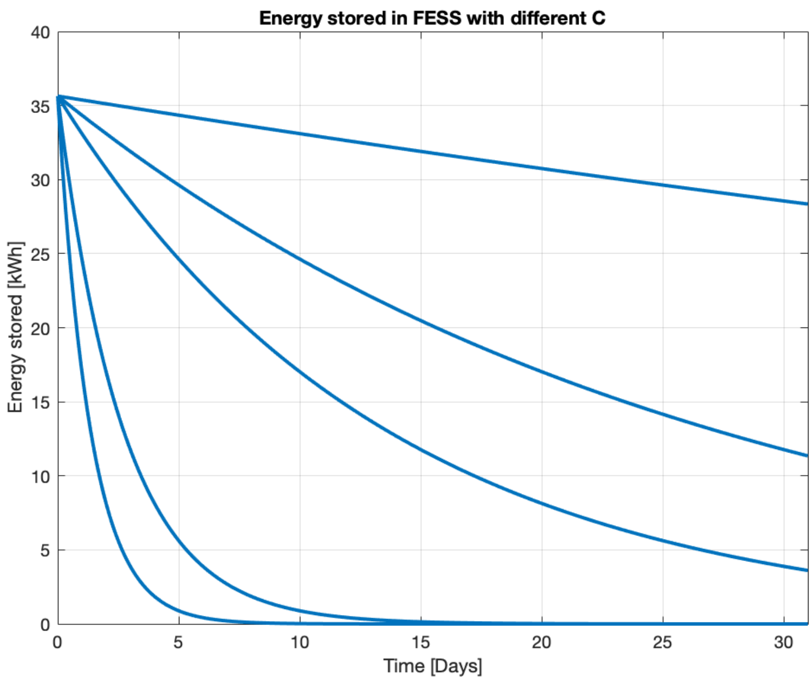

Figure 5.9: Spin out time of FESS with different resistance coefficient C.

Analyzing equation 4.11 together with equation 4.13 it is found that the torque lost due to the loss coefficient A is proportional to the rotational velocity cubed. The torque lost due to the coefficient B is proportional to the rotational velocity squared and from the coefficient C, is proportional to the rotational velocity. This is also seen in figure 5.9, figure 5.7 and figure 5.8. Here it is observed that the FESS with the coefficient A discharges faster although the coefficients simulated are smaller than for both B and C.

Storing the energy in the FESS over a longer period of time is essential, and is why FESS is kept in a low vacuum to reduce air resistance and often with magnetic bearings to reduce friction. The energy stored in a real FESS will usually dissipate within a few days due to losses. As data from real FESSs is very scarce, the values for the coefficients are only estimates and are used to show the effects of different types of losses. A real FESS would also include coefficients from all types of losses and as the simulated coefficients are isolated, it could be assumed that a real FESS would discharge faster.

5.2 Peak shaving

A simulation is performed to demonstrate how a FESS can contribute to lowering the power peaks on the electrical grid. A simple schematic describing the power flow in the scenario is displayed in figure 5.10. The load is connected to a grid which supplies the demanded power. A FESS is also connected to the load which can supply and draw power to and from the load when the power demand is above and below a certain limit. The code for the simulations are attached in Appendix D.

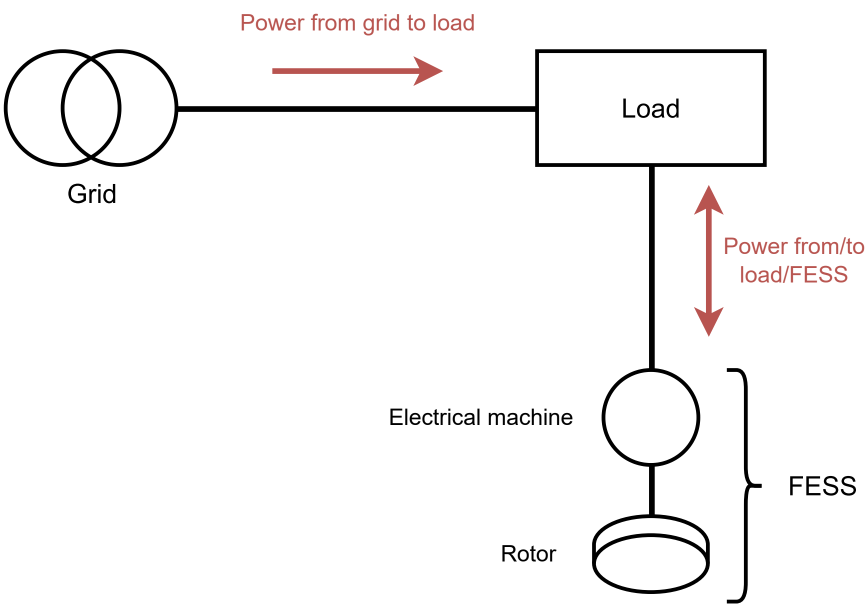

Figure 5.10: Schematic of peak shaving scenario.

In this simulation a 1300 kg solid cylinder FESS with a radius of 0.6 m is used to store and deliver power to the load. The FESS uses a PMSM with rated torque of 228 Nm. 10 000 RPM is the nominal speed of the machine and it is assumed a constant efficiency of 93 %. The flywheel has an initial rotational speed of 8000 RPM. The lower limit, where the FESS starts charging, is set at 100 W. Discharging of the FESS happens at the upper limit of 250 W. A model of daily consumption is made to match the profile of daily household demands [3].

To calculate the torque applied from the machine to the rotor, the power difference between the power demand and the shaving limits together with the rotational speed is used to calculate the torque using equation 4.14 and equation 4.15.

Figure 5.11 shows the effect the FESS has on the grid while peak shaving in the course of one day with the model for daily consumption. The energy stored in the FESS during this period is displayed in figure 5.12.

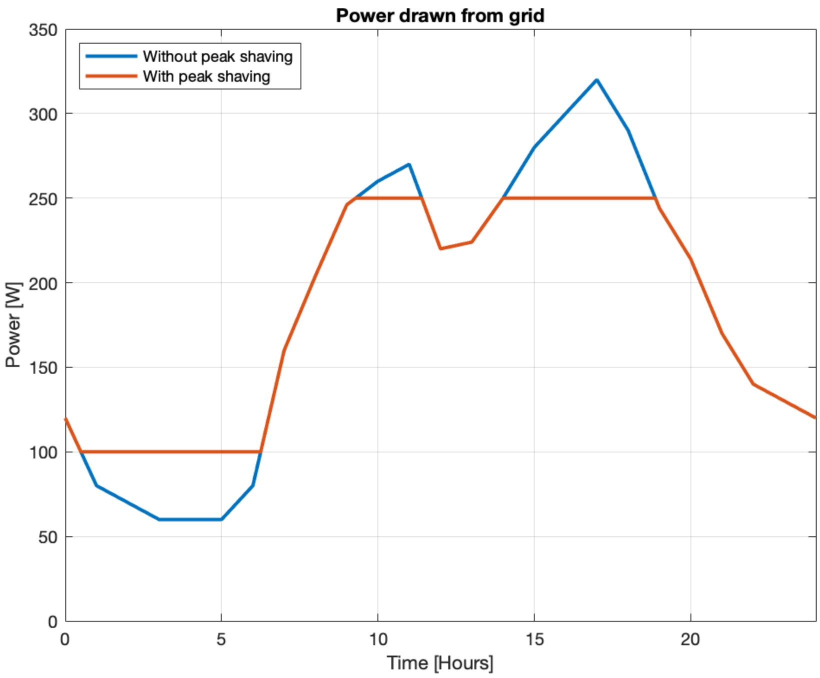

Figure 5.11: Power drawn from the grid by load with and without peak shaving for one day.

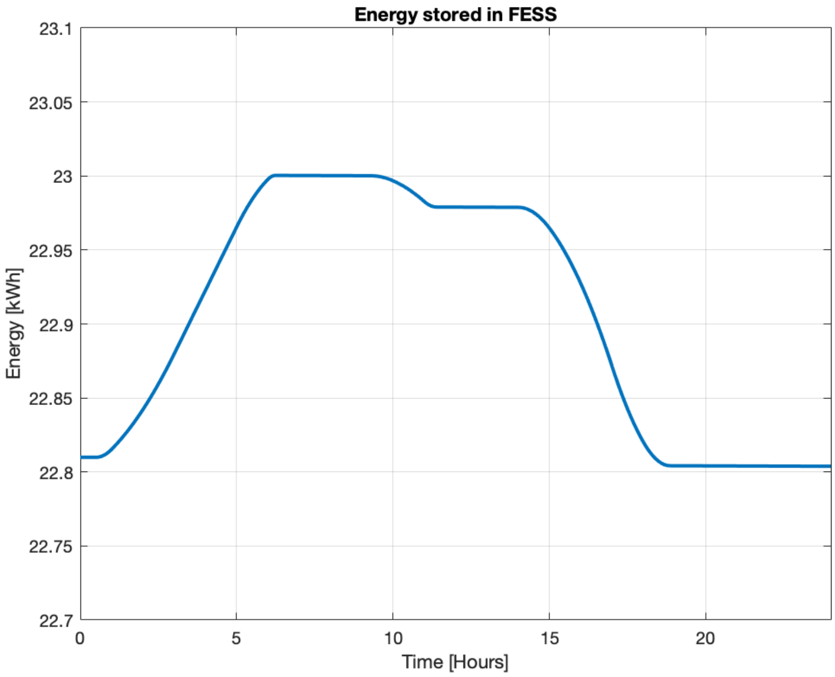

Figure 5.12: Energy stored in FESS while peak shaving for one day.

As observed in figure 5.11, the FESS successfully reduces the power peaks on the grid. This results in the highest peaks being about 30 % lower. If this is done at larger scales, a 30 % decrease of the highest power peaks on the grid has a big impact. It can result in grids not needing to be upgraded to meet the increase in power consumption and it will allow consumers to use more power at the same time.

If the demand would increase for a long duration of time and the desire of keeping the upper limit on the grid the same, the FESS would eventually run out of energy as it would need to discharge more than it is charging. A solution to this could be to increase the lower limit making the FESS charge more.

The scenario is repeated for the duration of a month. Each day the model for the daily power demand is multiplied with a randomly generated factor to create a fluctuating power demand throughout the month. Figure 5.13 shows the power drawn from the grid throughout the simulated month and figure 5.14 shows the stored energy in the FESS in the same period.

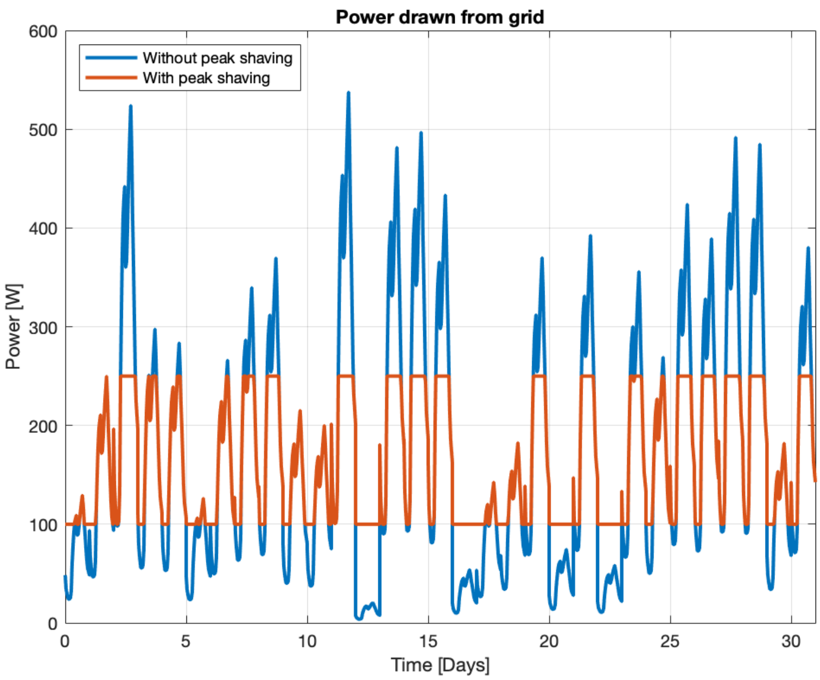

Figure 5.13: Power drawn from the grid by load with and without peak shaving for one month.

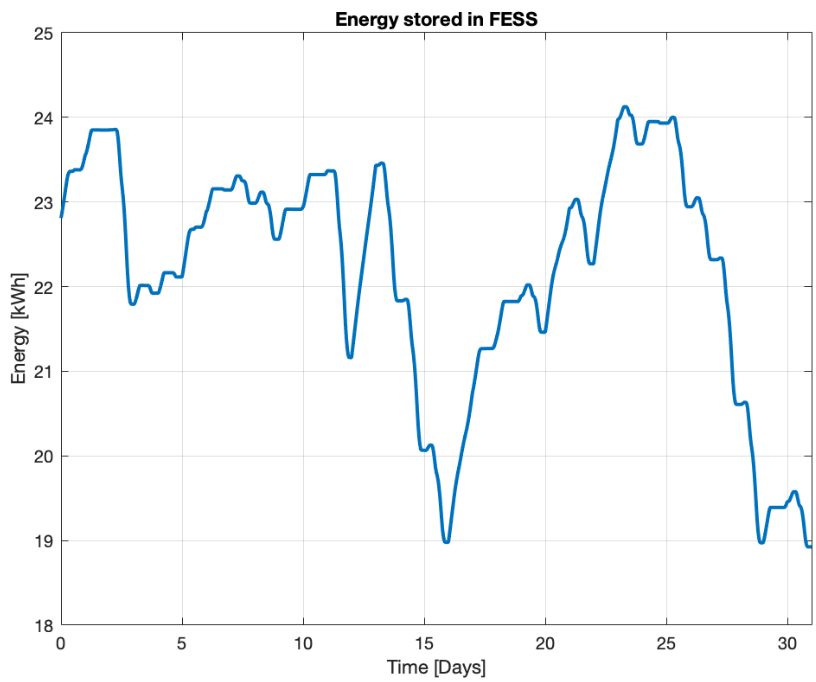

Figure 5.14: Energy stored in FESS while peak shaving for one month.

This case may showcase the effect the peak shaving has on the grid better. The peaks are higher and thus more of the peaks are shaved. The energy in the FESS fluctuates more than in the daily case. As observed in figure 5.14, the energy stored in the fess is quite a bit lower than what it started at, but a short period of lower peaks quickly increases the energy in the FESS as seen in the same figure on day 15.

In a more realistic case the power consumption would be quite a lot higher than in the simulations. If the FESS had to shave power on a bigger scale, the FESS would struggle to deliver the increased power for a longer period of time as the energy in the FESS would either quickly dissipate or charge to it max capacity.

5.3 Specific power output

In this scenario, it is investigated how a FESS can be used to achieve a specific, predictable and smooth power output to a load which is supplied with power from renewable energy sources. The simulations includes a case where the desired power input to the load is constant and a case where the power demand fluctuated throughout the day. The calculations and code for the simulations are attached in Appendix E.

The scenario consists of a wind turbine connected to a FESS and a load. The load can essentially be anything that draws power. A simple schematic of the scenario is shown in figure 5.15.

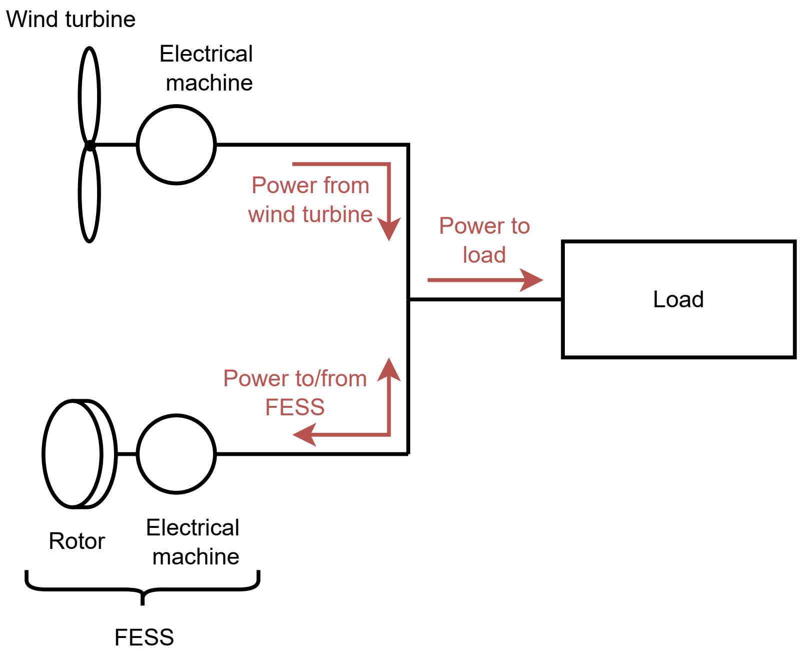

Figure 5.15: Schematic of specific power output scenario.

The FESS consists of a solid 1300 kg rotor with a radius of 0.6 m and the electric machine used in this FESS is a PMSM. The PMSM operates within its nominal speed of 10 000 RPM and it is assumed the electric machine operated with a constant efficiency of 93 %.

The wind speeds used in the simulations is gathered from *Norsk Klimaservicesenter*'s databases [28]. The data is from the weather station *Trondehim-Voll (SN68860)* from the 1st to the 31st of January 2023. In the simulations, it is assumed that the wind speeds stays constant for every 10 minutes as the smallest time resolution for the wind data is average wind speeds for every 10 minutes. *Raum Energy*'s 3.5 kW wind turbine system is the small scale wind turbine used to convert the kinetic energy in the wind to electric power [18]. The turbine's power curve together with the wind data is used to calculate the power output.

5.3.1 Constant power output

In this case, a FESS is used to achieve a constant power output so that the load will experience as close to a constant and predictable power input as possible.

Figure 5.16 shows the electric power produced from the wind turbine and the electric power absorbed and delivered by the FESS. Negative power from the FESS indicates the electric power that charges it, whilst positive values indicates the electric power delivered from it. The resultant power to the grid and delivered to the load is shown in figure 5.17.

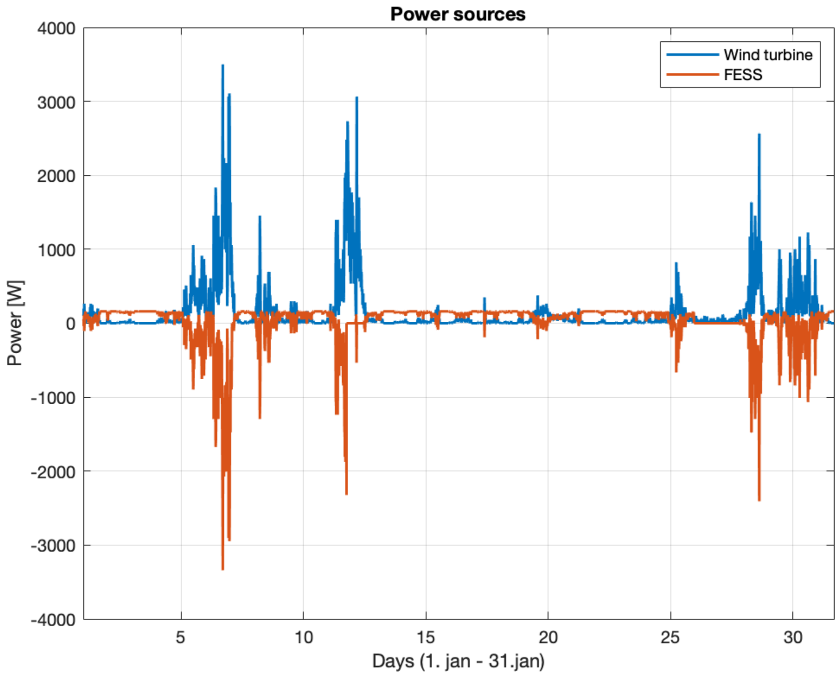

Figure 5.16: Electric power from wind turbine and FESS while supplying a load with 160 W.

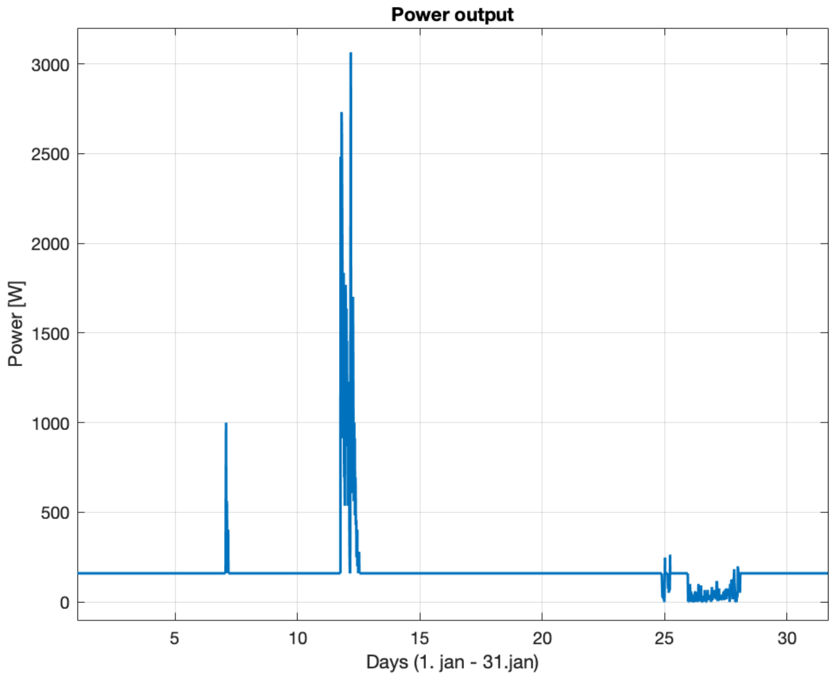

Figure 5.17: Electric power delivered to load while 160 W is desired.

The mechanical energy stored in the FESS during this period is shown in figure 5.18.

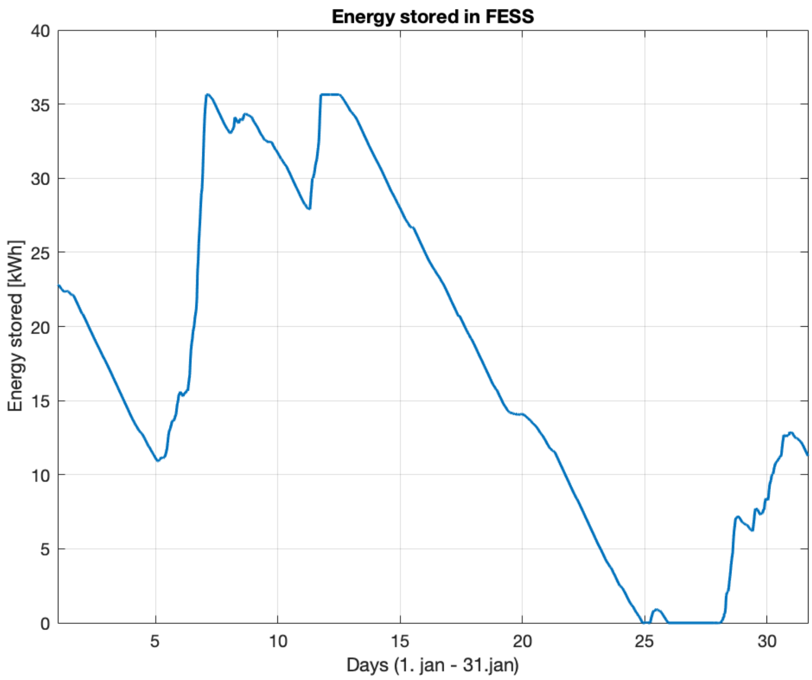

Figure 5.18: Energy stored in FESS while supplying constant power output of 160 W in conjunction with a wind turbine.

As observed in figure 5.17 the power output to the load is mostly constant, as desired, but there are a few power peaks. When analysing figure 5.17 together with figure 5.18, it is observed that the two first major positive power peaks, occurs around the 7th and 12th of January. These happen because the FESS has reached its rated speed and can therefore not charge any more. This caused the power from the wind turbine is to be directly transmitted to the load. Following, is a long period of little wind and the energy stored in the FESS decreases steadily until there is no power left. Around the 25th of January the power output drops due to low winds and no energy in the FESS. The power output then jumps above 160 W which is due to generated wind power being greater than the flywheel can receive at the low speeds. Right after, is another period of low winds before the wind steadily increases and the FESS charges up again.

This simulation showcases how a FESS can be used together with renewable energy sources to produce a stable and predictable power output. It also shows how it can be used as a UPS. As the power from the wind turbine drops below the desired power the FESS quickly engages and delivers the wanted power.

5.3.2 Fluctuating power demand

Another case is simulated, where the power demand fluctuates. A model for daily household consumption is used. Figure 5.19 shows the electrical power from the wind turbine and and the FESS during a one day period. The power delivered to the load during this period is shown in figure 5.20.

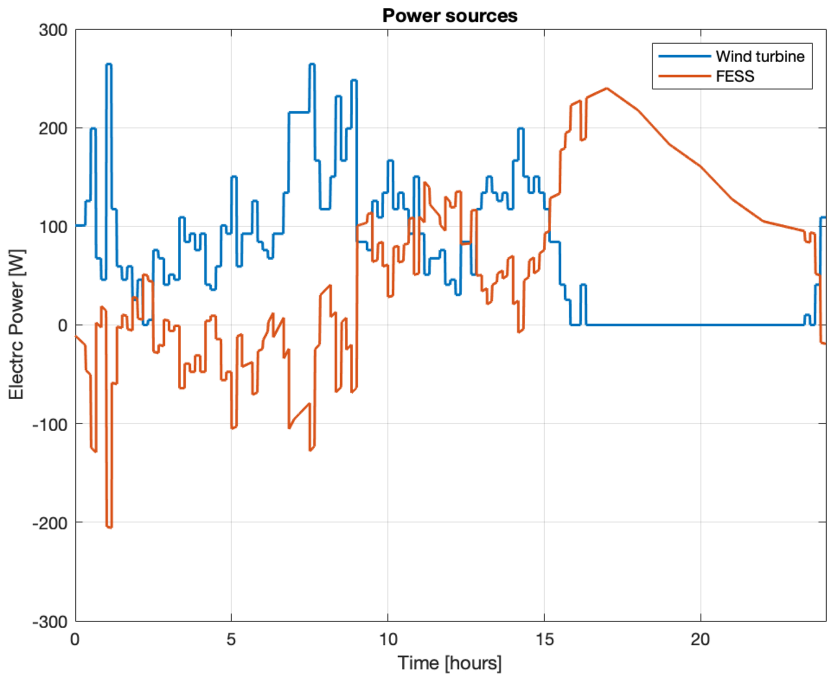

Figure 5.19: Electric power from wind turbine and FESS while supplying a fluctuating power output to the load for one day.

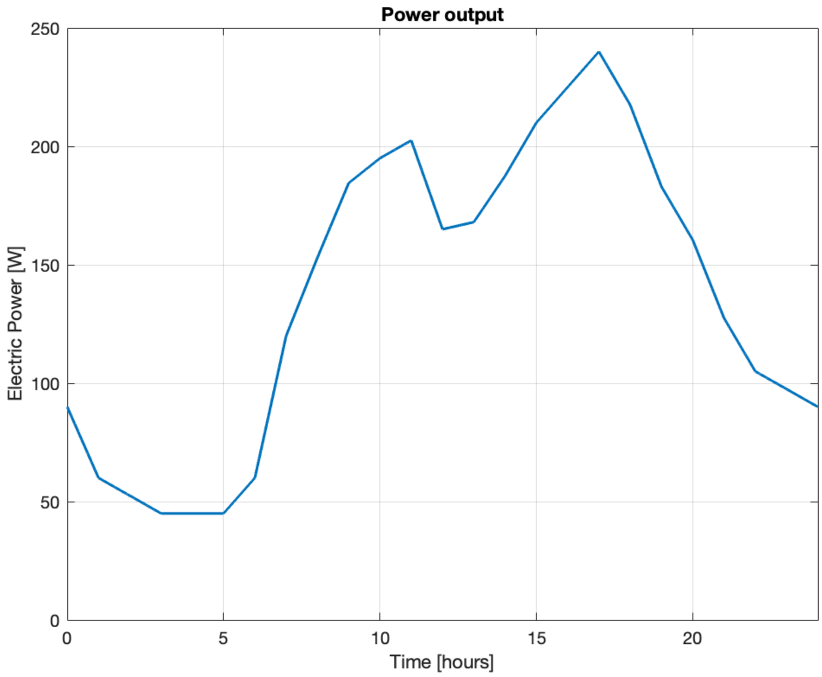

Figure 5.20: Electric power delivered to load while it has a fluctuating demand for one day.

Figure 5.21 shows the energy stored in the FESS during the simulated day.

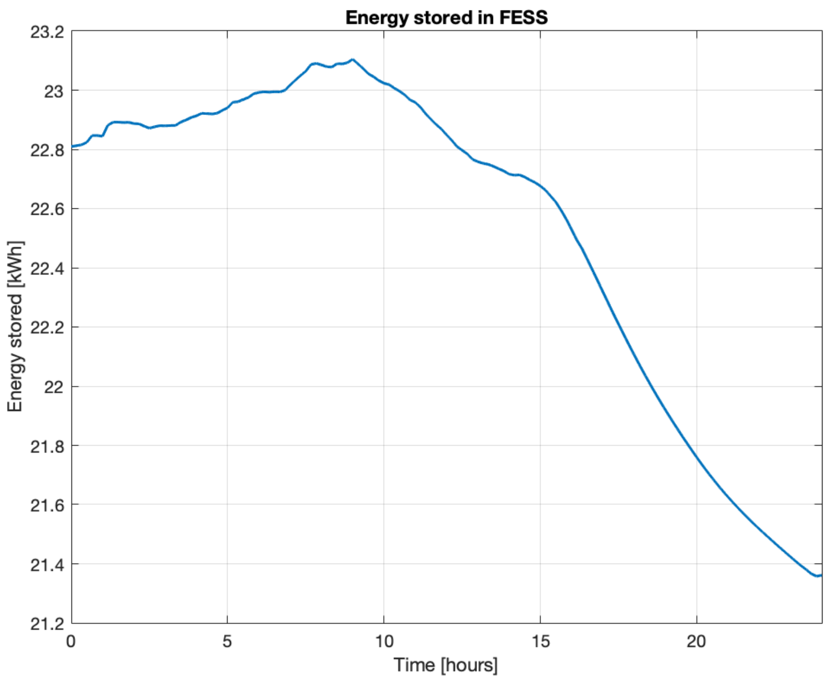

Figure 5.21: Energy stored in FESS while supplying a fluctuating power output in conjunction with a wind turbine for one day.

As observed in figure 5.21 the energy in the FESS drops substantially in the second half of the day due to the wind power being very low. Even though the power from the wind turbine is very low, the FESS has plenty of energy and is able to supply the needed power.

The simulation is repeated for a month. Figure 5.22 show the electric power from the wind turbine and the FESS. The power to the load is shown in figure 5.23.

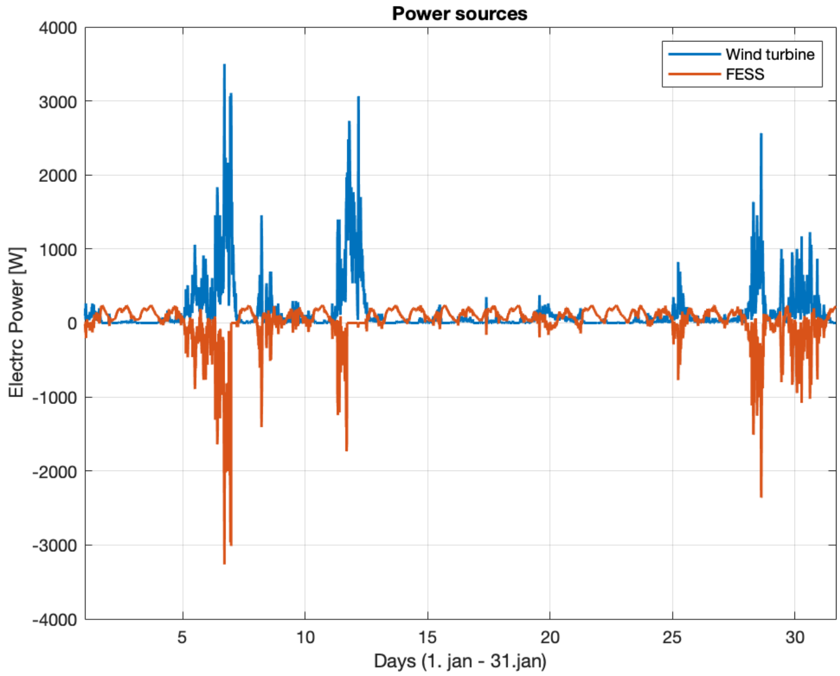

Figure 5.22: Electric power from wind turbine and FESS while supplying a fluctuating power output to the load for one month.

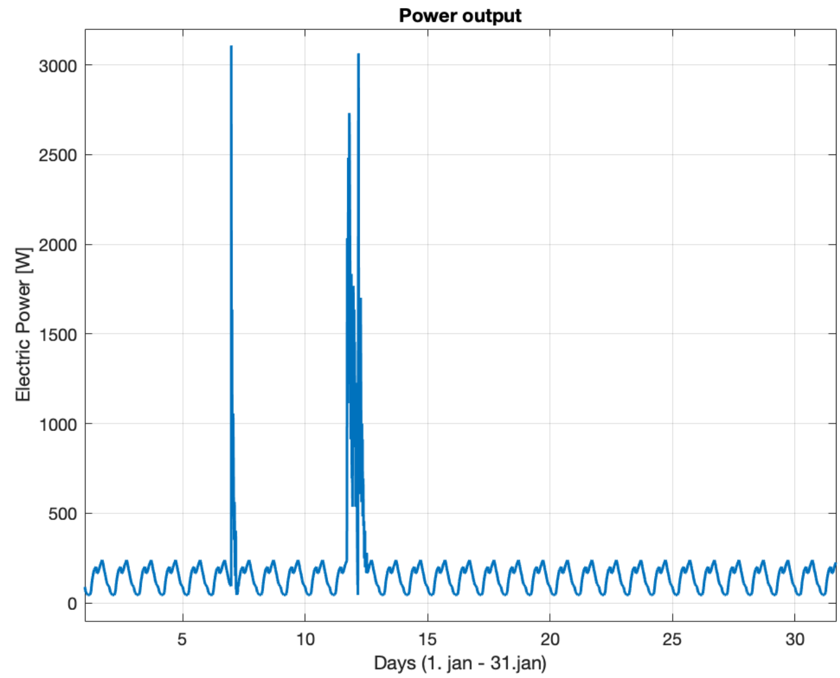

Figure 5.23: Electric power delivered to load while it has a fluctuating demand for one month.

Figure 5.24 shows the energy stored in the FESS during the simulated month.

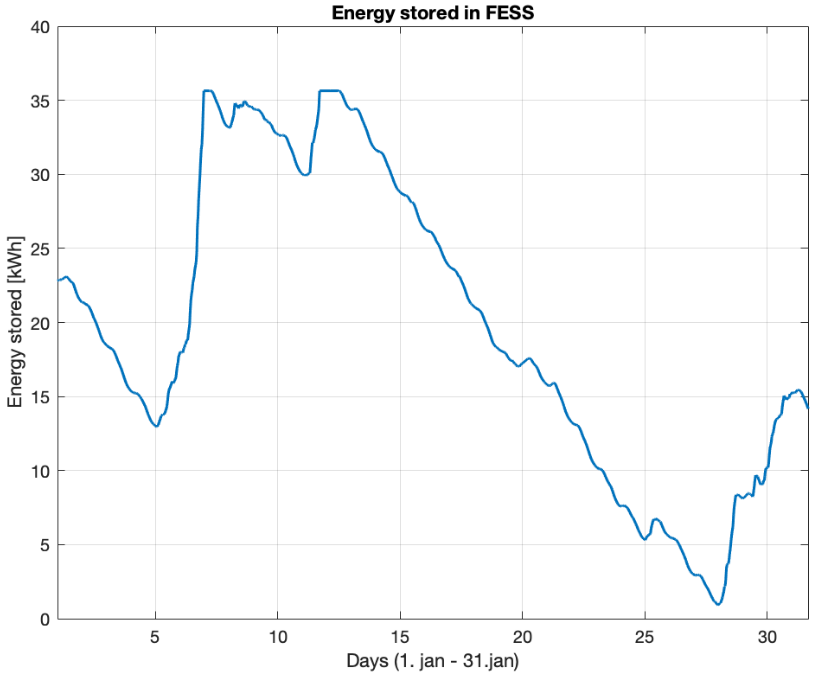

Figure 5.24: Energy stored in FESS while supplying a fluctuating power output in conjunction with a wind turbine for one month.

As observed in figure 5.23, the power to the load follows the desired demand during most periods of the month. But due to periods of high wind speeds, the FESS becomes fully charged and is therefore not able to draw more power from the grid. During the periods of low winds the FESS becomes nearly fully discharged. This means that in this case, the energy stored in the FESS is more important than the charging time. This means that a FESS with a heavier and bigger rotor would be more suitable.

5.4 Frequency control

In this scenario, a FESS is used to control the grid frequency. As the grid frequency has to be controlled very quickly, a PID controller is coupled with the FESS to make the electric machine operate smoothly and quickly. Figure 5.25 shows the scenario. It is the rotational speed of the electric machine in the turbine that is the only frequency source on this grid and is what determines the uncontrolled frequency. The MATLAB code used to simulate this scenario is attached in Appendix F.

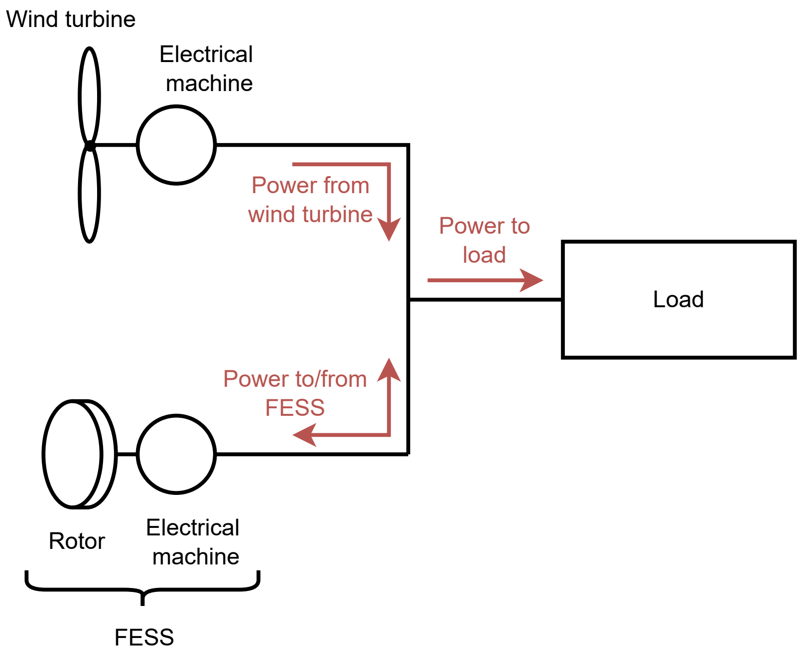

Figure 5.25: Schematic of frequency control scenario.

The FESS in this scenario consists of a 1300 kg solid cylinder rotor with a radius of 0.6 m and a PMSG that operated within its nominal speed of 10 000 RPM. The efficiency of the PMSG is assumed to be a constant 93 %. A wind turbine with 4 poles supplies the load with power. From equation 4.16, it is observed that when the rotor from this electrical machine rotates at a speed of 1500 RPM, it delivers a frequency of 50 Hz to the grid. The load in this scenario draws 3 MW which the wind turbine is able to supply.

Assuming the torque from the wind turbine is constant, the power from the wind turbine will increase as the demand, from the load, increases. Similarly it decreases as the demand decreases. The rotational speed of the wind turbine is proportional to the power of the wind turbine as seen in equation 4.15. In addition, the frequency is proportional to the rotational speed of the wind turbine as seen from equation 4.16. This means that the scenario essentially becomes a power balance between the turbine, the load and the FESS.

5.4.1 Tuning of controller

Figure 5.26 shows the closed feedback loop of the system. It includes the PID regulator, the FESS and a sensor for measuring the power in the grid. The power difference between the wind turbine and the load is modeled as a disturbance and the reference value is 0 W.

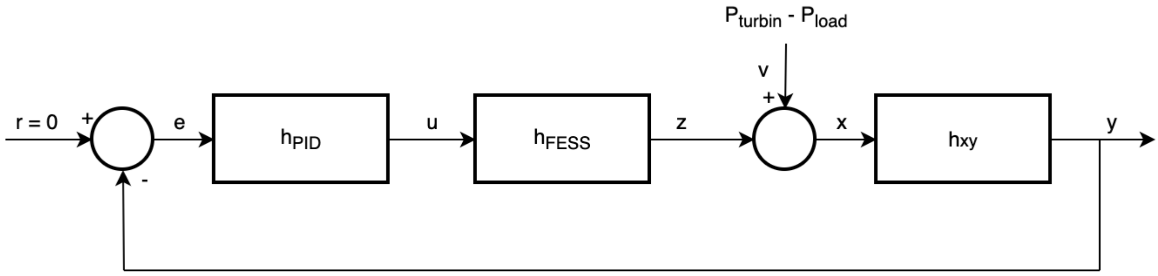

Figure 5.26: Closed feedback loop of system.

The electric machine in the FESS can deliver instant torque and it is assumed the FESS has enough power available to deliver instant power for short amounts of time. Therefore, its transfer function is only a time delay of 0.3 ms. The Laplace transformed transfer function for the FESS, h_{FESS}, is shown in equation 5.1. It can be assumed the instrument used to measure the power in the system also has a small delay without any dynamics. The transfer function for the measurement instrument, h_{xy}, is therefore the same as for the FESS as displayed in equation 5.2.

$$h_{FESS}(s) = 1 \cdot e^{-0.0003 \cdot s} \tag{5.1}$$

$$h_{xy}(s) = 1 \cdot e^{-0.0003 \cdot s} \tag{5.2}$$

The open loop of the uncontrolled system includes the transfer function of the FESS and the transfer function of the measurement instrument. Equation 5.3 shows the resultant Laplace transformed transfer function for the uncontrolled open loop.

$$h_0^*(s) = h_{FESS} \cdot h_{xy} = 1 \cdot e^{-0.0006 \cdot s} \tag{5.3}$$

Plotting the bode plot for equation 5.3 yields figure 5.27.

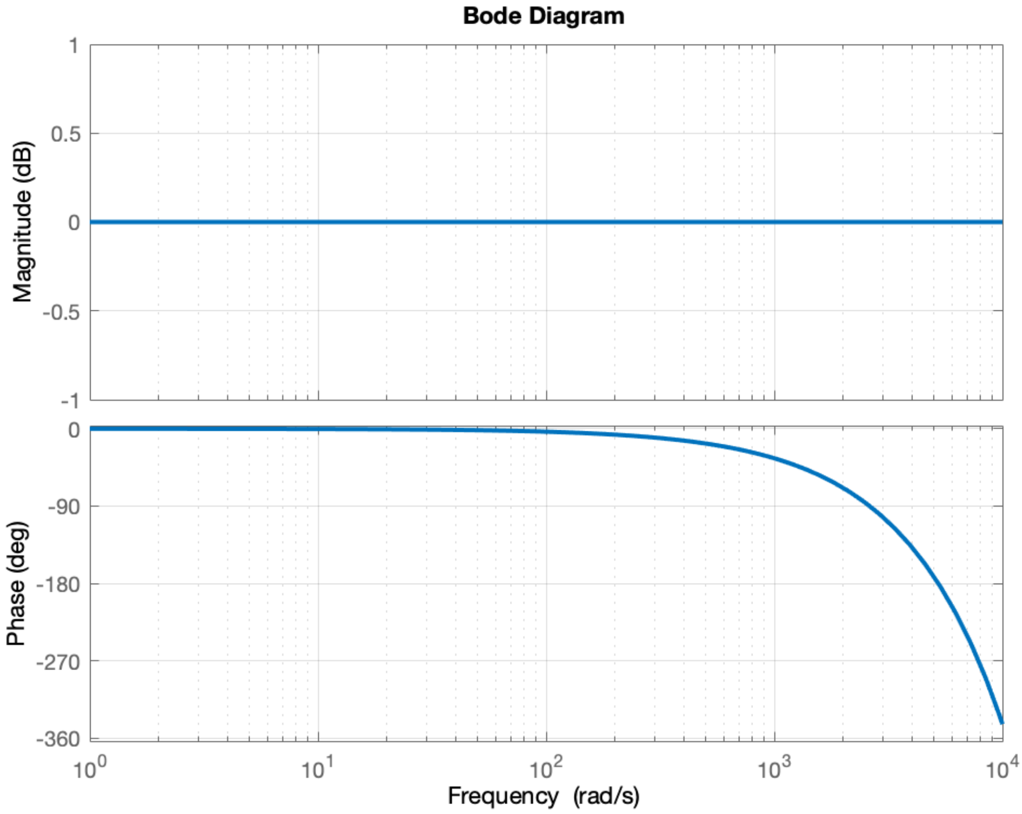

Figure 5.27: Bode plot of the open loop transfer function.

From figure 5.27 it is found that the wanted frequency, ω_w, at a phase angle of -155 ° is at 4500 rad/s and the magnitude, $\mid h_0^*(\omega_w) \mid_{dB}$, at this frequency is 0 dB. A minimum amplitude step response from the system is desired and the elements of the PID controller is tuned as such. A proposal for the tuning of each component of the controller is displayed in table 5.4.

Table 5.4: Proposal for tuning of PID controller.

PID parameter	**Expression**	**Value**
Kp	$\mid h_0^*(\omega_w) \mid_{dB}$ - 4 dB	(0 - 4) dB = 0.631
T_i	$2.8/\omega_w$	$2.8/4500 = 6.222 \cdot 10^{-4}$
T_d	$1/\omega_w$	$1/4500 = 2.222 \cdot 10^{-4}$

Inserting these values into equation 4.23, with $n = 10$, and multiplying with h_0^* yields a proposal for an open loop transfer function with the controller shown in equation 5.4.

$$h_{0,test}(s) = h_{PID} \cdot h_0^* \tag{5.4}$$

To test the stability of the system, a bode plot with the gain and phase margins as shown in figure 5.28.

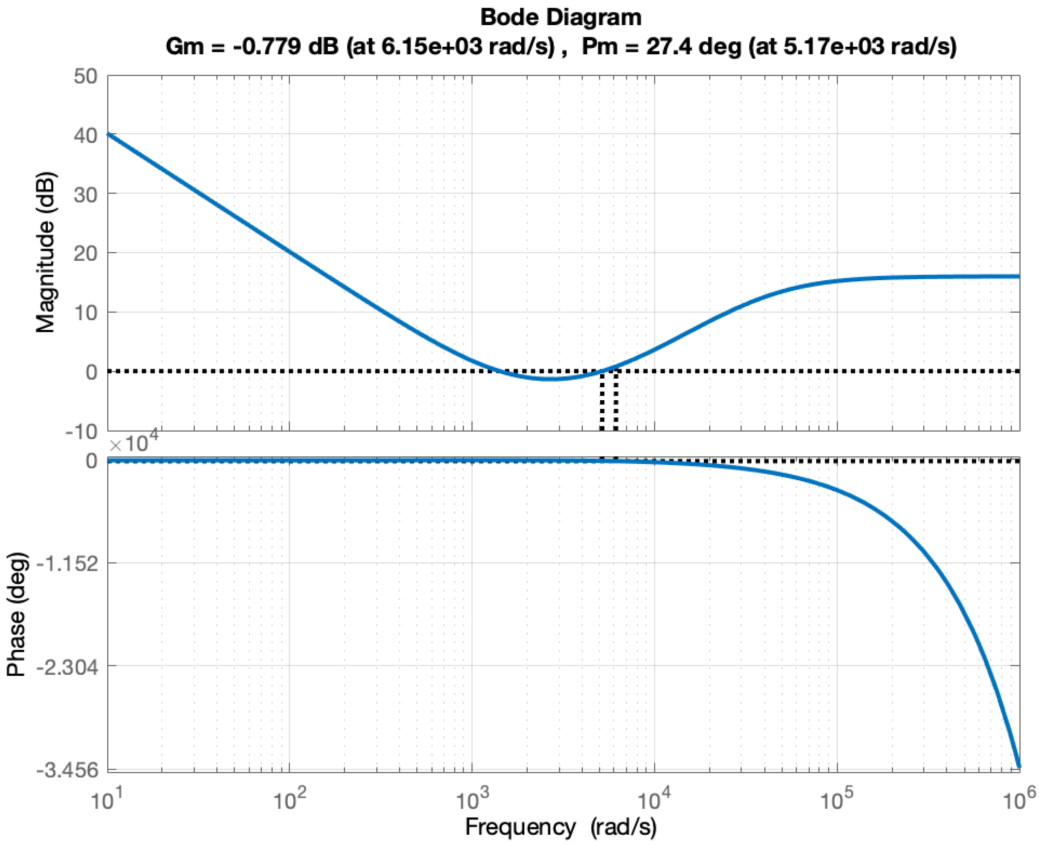

Figure 5.28: Margins to test the stability of the regulated system.

As seen in figure 5.28, both the gain and the phase margins are too small. The gain margin is -0.779 dB while for a minimum disturbance it is desired to have a gain margin of 12 dB. Adjusting the K_p such that the gain margin becomes equal to 12 dB results in the new tuning values as shown in table 5.5. The new margins are plotted in the bode plot shown in figure 5.29. Here both the gain and the phase margins are equal to or greater than the minimum requirements and the PID should be tuned properly and the system should be stable.

Table 5.5: Readjusted tuning of PID controller.

PID parameter	Test value	Readjusted value
Kp	-4 dB	-32 dB = 0.0251
T$_i$	$6.222 \cdot 10^{-4}$	$6.222 \cdot 10^{-4}$
T$_d$	$2.222 \cdot 10^{-4}$	$2.222 \cdot 10^{-4}$

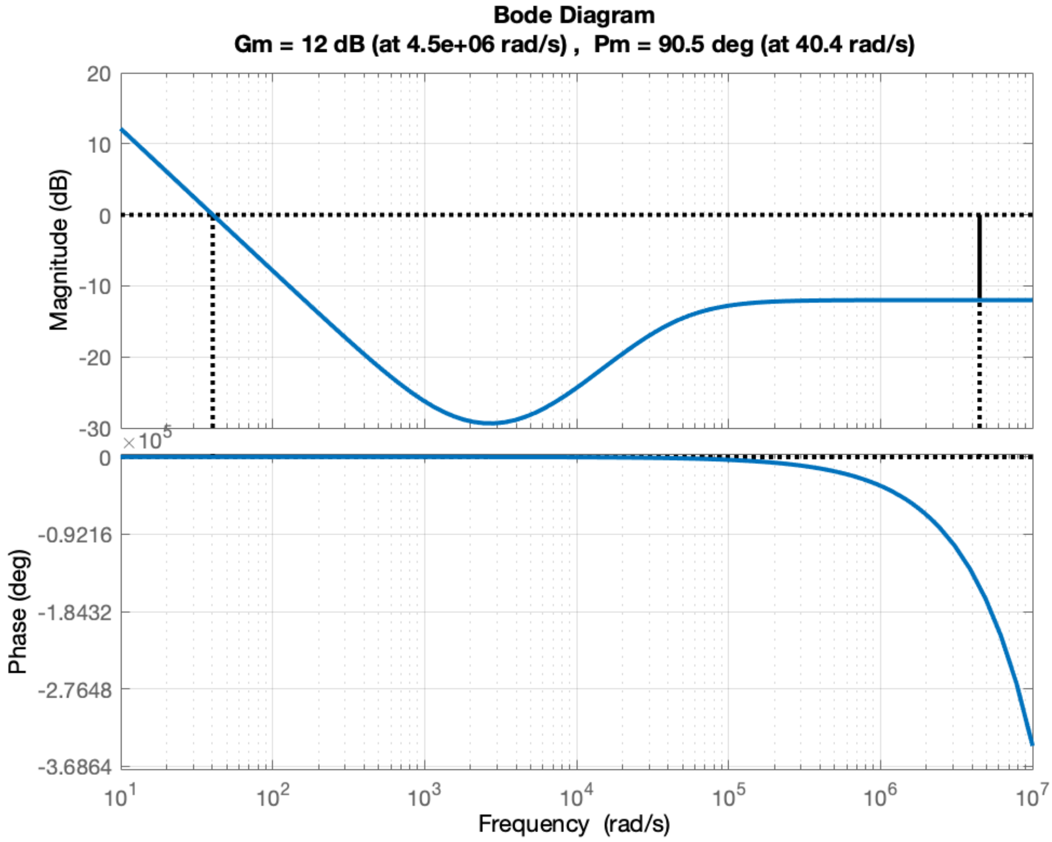

Figure 5.29: Readjusted margins of the regulated system.

To see the systems response to a disturbance, the step response of the transfer function between the disturbance and the measurement, h_{vy}, is plotted. This transfer function is shown in equation 5.5 where h_0 is described in equation 5.6. The step response of this transfer function is displayed in figure 5.30.

$$h_{vy} = \frac{h_{xy}}{1 + h_0} \tag{5.5}$$

$$h_0(s) = h_{PID} \cdot h_0^* \tag{5.6}$$

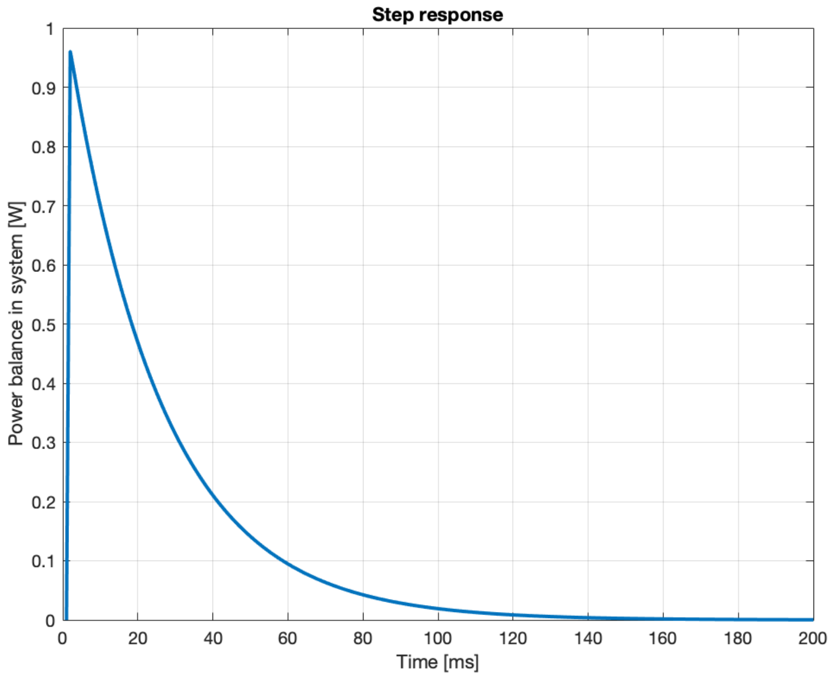

Figure 5.30: Response of controlled system when a step in the disturbance is applied.

As figure 5.30 shows, the FESS with the PID controller suppresses the power difference of the wind turbine and the load very smoothly within approximately 100 ms and with a time constant of about 25 ms. Increasing the derivation time, T_d, will increase the speed of the regulator but it will also decrease the stability of the system.

5.4.2 Grid frequency

Using the tuned PID controller together with the FESS, it is simulated how the grid frequency responds to the two arbitrary steps in the difference between the power from the wind turbine and load.

Figure 5.31 shows the frequency on the grid with and without frequency controlling with a FESS.

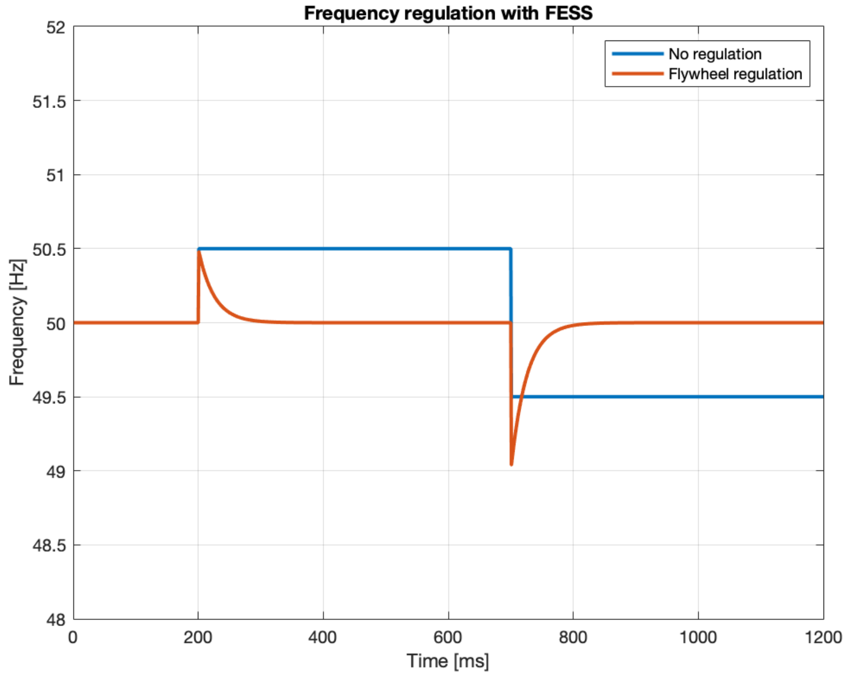

Figure 5.31: Frequency of the grid.

As observed in figure 5.31 the FESS responds quickly and the the frequency is smoothly stabilized back to 50 Hz. As seen in the same figure, around 700 ms, the FESS causes the frequency to deviate more than what it would do without the FESS. This is because the FESS is already drawing power from the grid and due to the small time delay continues to draw power. However this effect lasts only for a few milliseconds and the grid is quickly back to a steady 50 Hz. As seen, the unregulated frequency drops 1 Hz at an instant. Such a big fluctuation in the grid would rarely happen instantaneous, but rather over a small period of time. If this would be the case, the FESS would not cause that much of a deviation from 50 Hz, depending on how fast the change is.

Figure 5.32 shows the power flow in the system. Negative power on the FESS means it is charging while positive values means it is discharging and delivering power into the grid. The energy stored in the FESS is presented in figure 5.33.

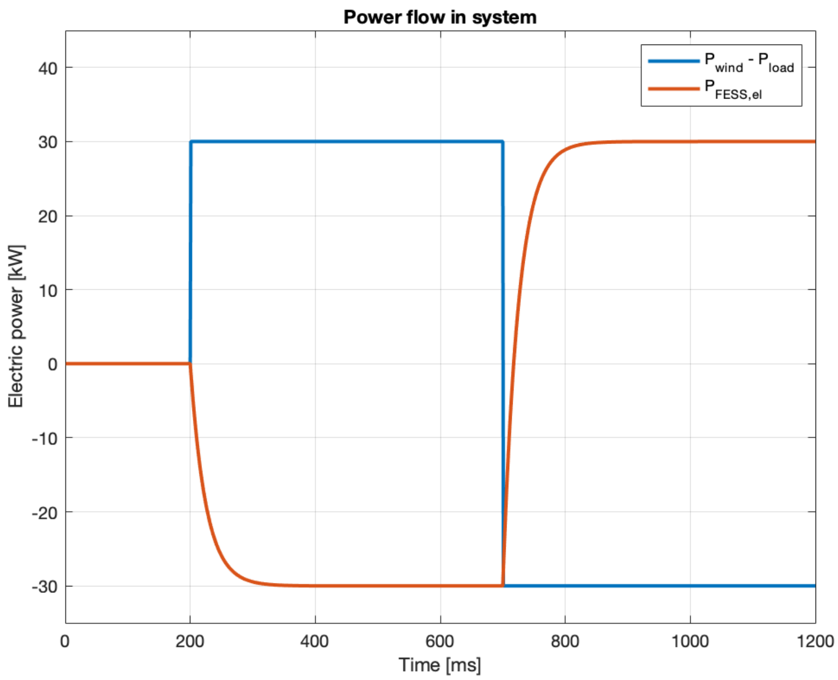

Figure 5.32: Power flow in system while grid frequency is regulated with FESS.

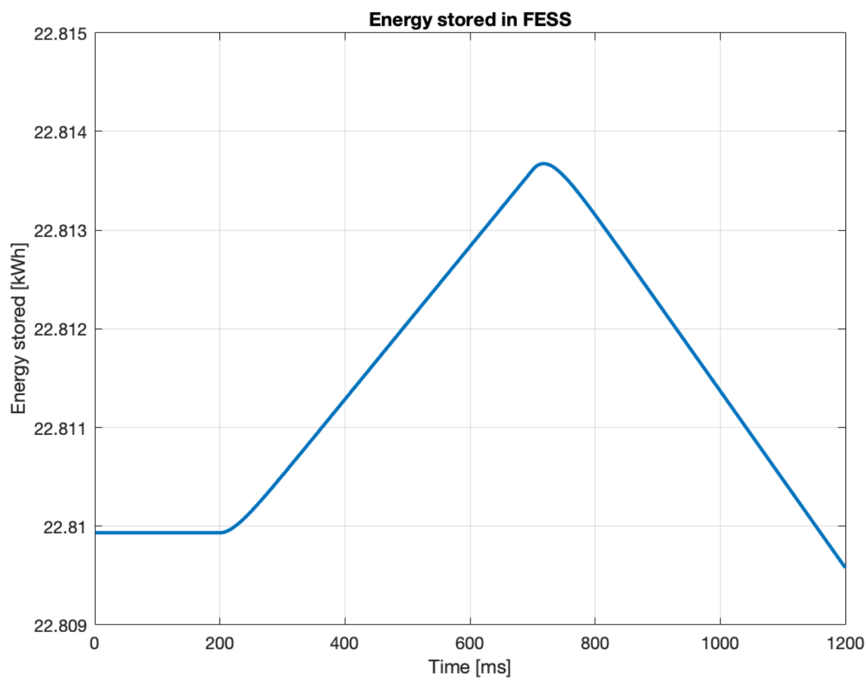

Figure 5.33: Energy stored in FESS while regulating grid frequency.

Figure 5.32 shows that the peak power the FESS has to deliver and draw, is 30 kW. As this simulation is only for 1.2 seconds, the change in energy is very small as seen in figure 5.33. The first step in frequency causes the FESS to charge less than 0.004 kWh and the second step causes the FESS to discharge a little bit more than 0.004 kWh. Even though both steps is frequencies deviates equally from 50 Hz and lasts for the same amount of time, the FESS discharges more than it charges due to the efficiency of the electric machine.

This scenario also show how a controller in a FESS is used, not only when it is used for frequency control but in essentially every scenario would include a control element in some way in the real world.

6 Discussion

In this section it is the more practical parts and uses of the FESS that will be discussed. This includes discussing what applications the FESS could perform well in, what materials to use, the cost comparison to lithium ion batteries, and the safety around the FESS.

6.1 Applications

While FESS has some limits, it certainly can be a useful tool in different applications presented earlier in this report. There are different situations where the FESS definitely excels. Looking at the larger picture one could maybe say that the widely used lithium ion batteries is a more flexible energy storage system. The FESS has a relatively low energy density, which means that it cannot store as much energy per unit of mass as other technologies such as lithium ion batteries. This makes FESS more suitable for applications that require high power output over short periods of time, rather than long-term energy storage. What FESS really has going for itself, is its ability to react extremely fast and its incredibly long life span. So for applications such as an UPS, grid frequency balancing or a voltage sag control, the FESS is a very suitable option. As for peak shaving or renewable energy integration the combination of FESS and another longer term energy storage system could be a viable solution to overcome these challenges. Quite a few FESSs has already been manufactured and are used in the applications mentioned earlier. For example, the incorporation of the FESS in the solar PV and diesel power stations in Western Australia boosted the PV system to provide 60 % of the average daytime energy shows that FESS can be a helpful energy storage system implementation.

6.2 Electric machine and materials

The round trip efficiency of a modern FESS is typically in the 90 % to 95 % range. The losses experienced in a FESS can become high if proper vacuum is not in place causing air drag on the rotor. This produces heat which reduces the kinetic energy in the rotor. This is especially noticeable when trying to store energy over a longer period. The efficiency also depends on the electric machines used in the FESS, as it experiences hysteresis and eddy current losses. As the FESS speed range varies, the optimal electric machine is not always the same and would need to be suited for each specific FESS.

There are quite a few characteristics that make the FESS an attractive option when talking about energy storage. Such as its very long lifespan, which could be anywhere from a hundred thousand to one million charge cycles. Furthermore, the FESS requires very little maintenance. Comparing this to a typical lithium ion battery with a estimated life time of 300-2000 charge cycles the FESS is superior. The materials used in a FESS is also non chemical, in the sense that there are no chemical reaction being used to store the electric energy. Both the composite materials as well as the steel used in commercial FESS are highly available. New and innovative steel based FESS designs has definitely increased the interest in steel based flywheels. Steel is easily recyclable compared to chemical batteries. Steel also has the benefit of already being a well established material, so the processing and transportation is well known and understood by the supply base.

The use of different bearings is an important factor when manufacturing a FESS. In the earlier days of the FESS, mechanical bearings was the bearing system used. These types of bearings creates a lot of frictional losses, especially when used in high speed FESSs. They also need lubrication and maintenance, which can be a nuisance when working in a close to vacuum environment. Therefore, in modern FESS's, magnetic bearings is the most likely bearing system to be used going forward. The hybrid system of passive magnetic bearings and active magnetic bearings is a good system. This is because the passive magnetic bearings are often cheaper, but inherently unstable. The active magnetic bearings can therefore be simpler than what is needed if used alone, but still counteract the unstability of the passive magnetic bearings.

6.3 Cost

The cost of the FESS is to date a lot higher than for example lithium ion batteries if capacity per dollar is what being compared. As mentioned earlier, the Beacon Power's FESS was around ten times more expensive than what a lithium ion battery power plant with the similar energy capacity would have been. That being said, FESSs is much less developed technology than the lithium ion batteries and their manufacturing scale is much smaller. Since the flywheel rotor are being heavily researched, especially composite rotors, it is possible that the research will find a type that increases the specific energy greatly which in itself is positive. On the other hand, the whole containment must be considered. The new composite rotors would most likely spin faster, meaning that the price of the MGPE presented in subsection 2.6 would increase. Since composite rotors failure models are not fully understood today, the housing of these composite rotors could also result in a higher cost if the research in the future shows that composite rotors are more explosive than initially thought. When the FESS increases in speed, it is all the more important to keep as close to an absolute vacuum as possible. This will probably also result in an increase in the cost, because of the pump frequency will go up or the sealing needs to be made even better than today.

6.4 Safety

While FESS seems to be a quite promising energy storage method, it is still a few properties that is not fully understood today. The major factor that probably rises the most scepticism to the common man is the safety of the FESS. As explained in subsection 2.5 there has been a few major incidents involving the failure of a FESS. Even though the FESS can cause fatal accidents, it is important to see that most of the accidents comes from neglect of safety. It is still not fully understood how different composite rotors actually fail, and they should be tested with caution and proper safety evaluation. To date, it seems that the most reliable method is to bury them underground so that the surrounding earth absorbs the energy from any possible failures. If further research on composite rotors helps us getting the full understanding of their failure modules, burst containment could perhaps be reduced without compromising the safety. Regarding the safety, it is no official safety procedure regarding installation of FESSs. It would probably help prevent accident considerably to insert an official safety procedure for producers to follow. A complication with this is that all FESS are quite different in energy capacity and power rating, so the safety instructions would probably need to be quite comprehensive. This requires a lot of research on the field, which again is money consuming as well as time consuming.

7 Conclusion

To conclude, the FESS is a storage system which is not heavily researched, but it has the potential to be a viable option in short term energy storage. As discussed earlier, there are some applications where the FESS really excels. This is for example as a UPS. The FESS's long life time and short charge/discharge time is great characteristics, as 97 % of all power disturbances lasts for less than three seconds. For sensitive loads, the FESS is a great tool to use as a voltage sag controller to keep the voltage in range of what is accepted by the loads even if the voltage fluctuations happens extremely fast.

To smooth out the output power of renewable energy such as wind and solar power, FESS can be used. Primarily in combination with other energy storage system which store energy over a longer period of time. Combining FESS with other energy storage systems is probably the best option for power peak shaving and grid frequency balancing as well.

The design of the FESS will vary depending on the application the FESS will be used. To conclude, composite rotors are definitely the type that has the highest specific energy and highest energy density. They are in return not fully understood and research is needed to understand what safety measures is needed when working with a composite rotor. When it comes to the bearings, a hybrid bearing system with active and passive magnetic bearings is the bearing system that results in the highest efficiency. This is also the system that most likely will be the most used in the future.

Throughout the simulations it was found that lighter and smaller rotor will charge faster but a heavier and larger FESS will have a greater energy storing capacity. It was also found that different electrical machines has different properties which is suitable in different applications and uses. It was also found how different types of losses affect the spin out time of a FESS and reducing the air drag will be the most important factor for increasing the spin out time. Simulating a FESS in different scenarios also revealed how the FESS could be used in different applications. It was found that in applications where an energy storage system needs to deliver and draw power quickly in small intervals suits the FESS the best.

8 Further work

For further work, it is suggested doing more comprehensive simulations including more realistic power electronics. Calculating the actual efficiency of the electric machines instead of using a constant efficiency could likewise be beneficiary. More realistic and complicated scenarios can be simulated by for example connecting the FESS to a larger and more realistic grid.

Research focusing on the material used in the flywheel rotor is an exciting field which has a lot of potential. Both in specific energy and energy density, as well as failure modules of different rotors. Testing failure modules of flywheel rotors needs to be done with high caution as accidents has happened before and potentially be lethal.

It is also suggested doing a deep dive looking into the costs of a FESS. This includes the system itself (rotor, MG, inverters, vacuum pump, housing, bearings), but also how much it is possible to earn by installing FESSs in various situations.

References

[1] 10News. *11K pound flywheel caused Poway explosion*. San Diego, Dec. 2015. URL: https://www.10news.com/news/11k-pound-flywheel-caused-poway-explosion (visited on 05/10/2023).

[2] ABB. *Regenerative drives and motors unlock the power of flywheel energy storage to stabilize Europe's grids*. en. July 2022. URL: https://new.abb.com/news/detail/93092/regenerative-drives-and-motors-unlock-the-power-of-flywheel-energy-storage-to-stabilize-europes-grids (visited on 05/11/2023).

[3] Jhud Mikhail Aberilla et al. *Design and environmental sustainability assessment of small-scale off-grid energy systems for remote rural communities*. Nov. 2019. URL: https://www.researchgate.net/publication/337512171_Design_and_environmental_sustainability_assessment_of_small-scale_off-grid_energy_systems_for_remote_rural_communities.

[4] Ajisman et al. *Study of Cooling Gases for Windage Loss Reduction*. 2000. DOI: 10.1541/ieejpes1990.120.3_478.

[5] Glen Alleman. *Is There an Underlying Theory of Software Project Management? (A critique of the transformational and normative views of project management)*. Oct. 2002. URL: https://www.researchgate.net/publication/2537163_Is_There_an_Underlying_Theory_of_Software_Project_Management_A_critique_of_the_transformational_and_normative_views_of_project_management.

[6] Mustafa E. Amiryar and Keith R. Pullen. *A Review of Flywheel Energy Storage System Technologies and Their Applications*. en. Mar. 2017. URL: https://www.mdpi.com/2076-3417/7/3/286 (visited on 03/07/2023).

[7] Amy. *Magnetic Bearings*. en-US. URL: https://www.kamansensors.com/industry/magnetic-bearings/ (visited on 05/19/2023).

[8] A.A. Khodadoost Arani et al. *Review of Flywheel Energy Storage Systems structures and applications in power systems and microgrids*. 2017. URL: https://www.sciencedirect.com/science/article/pii/S1364032116309054.

[9] Donald Bender. *Flywheels*. en-US. May 2015. URL: https://www.sandia.gov/ess-ssl/publications/SAND2015-3976.pdf (visited on 03/08/2023).

[10] Donald Arthur Bender. *Recommended Practices for the Safe Design and Operation of Flywheels*. Dec. 2015. URL: https://www.osti.gov/biblio/1331512.

[11] J.G. Bitterly. *Flywheel technology past, present, and 21st Century projections*. July 1997. DOI: 10.1109/IECEC.1997.658228.

[12] Kåre Bjørvik and Per Hveem. *Reguleringsteknikk*. nb. Kybernetes forlag, Aug. 2014. ISBN: 978-82-92986-21-9.

[13] BYJUS. *Laplace Transform*. en. Oct. 2020. URL: https://byjus.com/maths/laplace-transform/ (visited on 05/19/2023).

[14] Yung-kang Chin. *A PERMANENT MAGNET SYNCHRONOUS MOTOR FOR AN ELECTRIC VEHICLE - DESIGN ANALYSIS*. en. 2004. URL: http://kth.diva-portal.org/smash/get/diva2:7754/FULLTEXT01.pdf.

[15] All about circuits. *Synchronous Motors*. en. URL: https://www.allaboutcircuits.com/textbook/alternating-current/chpt-13/synchronous-motors/ (visited on 05/08/2023).

[16] Mohamed I. Daoud et al. *A Flywheel Energy Storage System for Fault Ride Through Support of Grid-Connected VSC HVDC-Based Offshore Wind Farms*. Conference Name: IEEE Transactions on Power Systems. May 2016. DOI: `10.1109/TPWRS.2015.2465163`.

[17] Kiran Daware. *What is an electrical machine?* URL: `https://www.electricaleasy.com/2012/12/what-is-electrical-machine.html` (visited on 05/11/2023).

[18] Raum Energy. *3.5 kW Wind Turbine System Specification Sheet*. URL: `https://farm-energy.extension.org/wp-content/uploads/2019/04/3.5kW_Spec_Sheet.pdf` (visited on 04/28/2023).

[19] David Flint. *Eastern Rensselaer County's Community Newspaper*. URL: `https://eastwickpress.com/news/2011/07/a-mishap-at-the-beacon-power-frequency-flywheel-plant/` (visited on 05/08/2023).

[20] S. M. Mousavi G et al. *A comprehensive review of Flywheel Energy Storage System technology*. 2017. DOI: `https://doi.org/10.1016/j.rser.2016.09.060`. URL: `https://www.sciencedirect.com/science/article/pii/S1364032116305597`.

[21] Ahmed Ghoniem. *Needs, resources and climate change: Clean and efficient conversion technologies — Elsevier Enhanced Reader*. en. Apr. 2010. URL: `https://reader.elsevier.com/reader/sd/pii/S0360128510000341?token=54B984F43DF1E1E16C67C16BB5D85451A3968E4693A562AC7219FFA115B3427FA4C90C04602EEA830595BDC5F65F7F2C&originRegion=eu-west-1&originCreation=20230425170718` (visited on 04/25/2023).

[22] EEE Guide. *Switched Reluctance Motor*. en-US. Jan. 2019. URL: `https://www.eeeguide.com/switched-reluctance-motor/` (visited on 05/09/2023).

[23] N Hamsic et al. *Stabilising the Grid Voltage and Frequency in Isolated Power Systems Using a Flywheel Energy Storage System*. Mar. 2023. URL: `https://www.researchgate.net/publication/268048579_Stabilising_the_Grid_Voltage_and_Frequency_in_Isolated_Power_Systems_Using_a_Flywheel_Energy_Storage_System` (visited on 03/06/2023).

[24] R. Hebner, J. Beno, and A. Walls. *Flywheel batteries come around again*. Conference Name: IEEE Spectrum. Apr. 2002. URL: `https://ieeexplore.ieee.org/stamp/stamp.jsp?tp=&arnumber=993788` (visited on 03/07/2023).

[25] Magnus Hedlund et al. "Flywheel Energy Storage for Automotive Applications". In: *Energies* 8 (Sept. 2015), pp. 10636–10663. DOI: `10.3390/en81010636`.

[26] Jens-s. *Vinkel kontakt kulelager*. URL: `https://www.jens-s.no/produkter/lager/kulelager/vinkel-kontakt-kulelager/` (visited on 05/19/2023).

[27] Jonathan Spencer Jones. *The different types of energy storage and their opportunities*. en. May 2021. URL: `https://www.smart-energy.com/storage/the-different-types-of-energy-storage-and-their-opportunities/` (visited on 05/08/2023).

[28] Norsk Klimaservicesenter. *Observasjoner og værstatistikk - Seklima*. URL: `https://seklima.met.no/` (visited on 04/28/2023).

[29] Elias Korsnes et al. *Flywheel Energy Storage System*. en. 2022.

[30] D P Kothari and I J Nagrath. *Electric Machines*. en. Fifth edition. McGraw Hill, 2020. ISBN: 978-93-5260-640-5.

[31] Wenlong Li et al. *Design and Analysis of a Flux-Controllable Linear Variable Reluctance Machine*. Conference Name: IEEE Transactions on Applied Superconductivity. June 2014. DOI: `10.1109/TASC.2013.2284720`.

[32] Xiaojun Li and Alan Palazzo. *A review of flywheel energy storage systems: state of the art and opportunities — Elsevier Enhanced Reader*. en. Dec. 2021. DOI: `10.1016/j.est.202

1.103576. URL: https://www.sciencedirect.com/science/article/pii/S2352152X2101255X (visited on 03/07/2023).

[33] Haichang Liu and Jihai Jiang. *Flywheel energy storage—An upswing technology for energy sustainability*. 2007. URL: https://www.sciencedirect.com/science/article/pii/S0378778806002350.

[34] Haichang Liu and Jihai Jiang. *Flywheel energy storage—An upswing technology for energy sustainability*. 2007. URL: https://www.sciencedirect.com/science/article/pii/S0378778806002350.

[35] msubbu. *Block Diagram Reduction*. en. Feb. 2022. URL: https://msubbu.in/sp/ctrl/BD-Rules.htm (visited on 05/19/2023).

[36] NREL. *NREL Analysis Explores Demand-Side Impacts of a Highly Electrified Future*. en. July 2018. URL: https://www.nrel.gov/news/program/2018/analysis-demand-side-electrification-futures.html (visited on 05/07/2023).

[37] Rickard Östergård. *Flywheel energy storage : a conceptual study*. eng. 2011. URL: http://urn.kb.se/resolve?urn=urn:nbn:se:uu:diva-164500 (visited on 04/18/2023).

[38] R. Peña-Alzola et al. *Review of flywheel based energy storage systems*. May 2011. DOI: 10.1109/PowerEng.2011.6036455.

[39] R. Peña-Alzola et al. *Review of flywheel based energy storage systems*. 2011. DOI: 10.1109/PowerEng.2011.6036455.

[40] Beacon Power. *Carbon Fiber Flywheels*. 2018. URL: https://beaconpower.com/carbon-fiber-flywheels/ (visited on 04/24/2023).

[41] Beacon Power. *Operating Plants*. 2018. URL: https://beaconpower.com/operating-plants/ (visited on 03/06/2023).

[42] Beacon Power. *Stephentown, New York*. 2018. URL: https://beaconpower.com/stephentown-new-york/ (visited on 03/06/2023).

[43] Keith R. Pullen. *The Status and Future of Flywheel Energy Storage*. 2019. URL: https://www.sciencedirect.com/science/article/pii/S2542435119302041.

[44] Hannah Ritchie and Pablo Rosado. *Energy: Key Charts*. Dec. 2021. URL: https://ourworldindata.org/energy-key-charts (visited on 05/07/2023).

[45] T. Rudnicki et al. *Performance analysis of a PMSM drive with torque and speed control*. June 2015. URL: https://www.researchgate.net/publication/308821510_Performance_analysis_of_a_PMSM_drive_with_torque_and_speed_control#pf2.

[46] A. Rupp et al. *Analysis of a flywheel energy storage system for light rail transit*. en. July 2016. URL: https://www.sciencedirect.com/science/article/pii/S0360544216304571 (visited on 03/08/2023).

[47] Oliver Schmidt et al. *Projecting the Future Levelized Cost of Electricity Storage Technologies*. 2019. URL: https://www.sciencedirect.com/science/article/pii/S254243511830583X.

[48] R Sebastian and R Pena Alzola. *Flywheel energy storage systems Review and simulation for an isolated wind power system*. en. Aug. 2012. URL: https://www.sciencedirect.com/science/article/pii/S1364032112004777 (visited on 03/06/2023).

[49] Siemens. *Ireland's great grid stabilizer*. en. Nov. 2022. URL: https://www.siemens-energy.com/global/en/news/magazine/2022/irelands-great-grid-stabilizer.html (visited on 05/11/2023).

[50] Siemens. *The right momentum for grid stability*. en. Nov. 2021. URL: https://www.siemens-energy.com/global/en/news/magazine/2021/flywheels-for-electranet-substation.html (visited on 05/11/2023).

[51] AE Solar. *Peak shaving - Off grid system*. en-US. June 2021. URL: https://ae-solar.com/peak-shaving-off-grid-system/ (visited on 05/08/2023).

[52] *System balancing*. URL: https://www.50hertz.com/en/Grid/Systemcontrol/Systembalancing (visited on 05/19/2023).

[53] Electrical Technology. *Torque-Speed Characteristics of Induction Motor*. en-US. Apr. 2022. URL: https://www.electricaltechnology.org/2022/04/torque-slip-torque-speed-characteristics-induction-motor.html (visited on 05/09/2023).

[54] Eric Tegler. *Why did the flywheel hybrid system never catch on for road cars?* en-us. Feb. 2021. URL: https://arstechnica.com/cars/2021/02/whatever-happened-to-williams-f1s-flywheel-hybrid-idea/ (visited on 05/20/2023).

[55] UCSUSA. *Let's Upgrade the Electricity Grid*. en. Feb. 2017. URL: https://www.ucsusa.org/resources/lets-upgrade-electricity-grid (visited on 05/08/2023).

[56] VYCON. *Run Times & Specs*. en-US. URL: https://vyconenergy.com/products/ups/run-times-specs/ (visited on 03/07/2023).

[57] Wikimedia. *Thinktank Birmingham - Trevithick Locomotive*. en. Aug. 2005. URL: https://commons.wikimedia.org/wiki/File:Thinktank_Birmingham_-_Trevithick_Locomotive(1).jpg (visited on 05/08/2023).

[58] Jiancheng Zhang et al. *Flywheel energy storage system design for distribution network*. 2000. DOI: 10.1109/PESW.2000.847295.

[59] Long Zhou and ZhiPing Qi. *Modeling and simulation of flywheel energy storage system with IPMSM for voltage sags in distributed power network*. 2009. DOI: 10.1109/ICMA.2009.5246111.

A Appendix A: Different rotors code

```
close all; clear; clc;

%------------Different rotor shapes------------
%Flywheel rotor 1: solid cylinder
r1 = 0.6; %radius [m]
m1 = 1300; %mass [kg]
I1 = 0.5*m1*r1^2; %moment of inertia [kg m^2]

%Flywheel rotor 2: Hollow cylinder (thin rim)
r2_inner = 0.45; %inner radius [m]
r2_outer = 0.6; %outer radius [m]
m2 = 1300 - 1300*(r2_inner^2 / r2_outer^2); %mass [kg]
I2 = 0.5*m2*(r2_inner^2 + r2_outer^2);  %moment of inertia [kg m
   ^2]

%Flywheel rotor 2: Hollow cylinder (thick rim)
r3_inner = 0.3; %inner radius [m]
r3_outer = 0.6; %outer radius [m]
m3 = 1300 - 1300*(r3_inner^2 / r3_outer^2); %mass [kg]
I3 = 0.5*m3*(r3_inner^2 + r3_outer^2);  %moment of inertia [kg m
   ^2]

%Electric machine
T_rated = 228; %Constant torque [Nm]
n_rated = 9000; %rated speed
R = 0.0000001; %Constant resistance factor

%Initial angular momentum
L1 = [0];
L2 = [0];
L3 = [0];

%Charging the FESSs for 1000 seconds
for i = 2:1:1000
    L1(i) = dpdt(L1(i-1), I1, T_rated, R);
    L2(i) = dpdt(L2(i-1), I2, T_rated, R);
    L3(i) = dpdt(L3(i-1), I3, T_rated, R);
end

%Calculating the energy and speed of the FESSs
E1 = 0.5.*(L1.^2)./I1 .* (2.7778 *10^(-7));
n1 = L1./I1 .* (60/(2*pi));

E2 = 0.5.*(L2.^2)./I2 .* (2.7778 *10^(-7));
n2 = L2./I2 .* (60/(2*pi));
```

```
E3 = 0.5.*(L3.^2)./I3 .* (2.7778 *10^(-7));
n3 = L3./I3 .* (60/(2*pi));

%Plotting the energy stored in the FESS
plot(E1, "LineWidth",2)
title("Energy stored in FESS while charging")
xlabel("Time [s]")
ylabel("Stored energy [kWh]")
hold on
plot(E2, "LineWidth",2)
plot(E3, "LineWidth",2)
grid
legend(["Solid cylinder", "Thin rim", "Thick rim"], 'Location','
    northwest')
ylim([0 30])
hold off

%Plotting the speed od the FESS
plot(n1, "LineWidth",2)
title("Rotor speed of FESS while charging")
xlabel("Time [s]")
ylabel("Rotor speed [rpm]")
hold on
plot(n2, "LineWidth",2)
plot(n3, "LineWidth",2)
grid
legend(["Solid cylinder", "Thin rim", "Thick rim"], 'Location','
    northwest')
ylim([0 10000])
hold off

%------------Different rotor masses------------
%Flywheel rotor 1: solid cylinder
r1 = 0.6; %radius [m]
m1 = 1300; %mass [kg]
I1 = 0.5*m1*r1^2;  %moment of inertia [kg m^2]

%Flywheel rotor 2: solid cylinder
r2 = 0.6; %radius [m]
m2 = 1600; %mass [kg]
I2 = 0.5*m2*r2^2;  %moment of inertia [kg m^2]

%Flywheel rotor 3: solid cylinder
r3 = 0.9; %radius [m]
m3 = 1300; %mass [kg]
I3 = 0.5*m3*r3^2;  %moment of inertia [kg m^2]
```

```

%Flywheel rotor 4: solid cylinder
r4 = 0.9; %radius [m]
m4 = 1600; %mass [kg]
I4 = 0.5*m4*r4^2;  %moment of inertia [kg m^2]

%Initial angular momentum
L1 = [0];
L2 = [0];
L3 = [0];
L4 = [0];

%Charging FESSs for 3000 seconds
for i = 2:1:3000
    L1(i) = dpdt(L1(i-1), I1, T_rated, R);
    L2(i) = dpdt(L2(i-1), I2, T_rated, R);
    L3(i) = dpdt(L3(i-1), I3, T_rated, R);
    L4(i) = dpdt(L4(i-1), I4, T_rated, R);
end

%Calculating energy and speed of FESSs
E1 = 0.5.*(L1.^2)./I1 .* (2.7778 *10^(-7));
n1 = L1./I1 .* (60/(2*pi));

E2 = 0.5.*(L2.^2)./I2 .* (2.7778 *10^(-7));
n2 = L2./I2 .* (60/(2*pi));

E3 = 0.5.*(L3.^2)./I3 .* (2.7778 *10^(-7));
n3 = L3./I3 .* (60/(2*pi));

E4 = 0.5.*(L4.^2)./I4 .* (2.7778 *10^(-7));
n4 = L4./I4 .* (60/(2*pi));

%Plotting energy stored in the FESSs
plot(E1, "LineWidth",2)
title("Energy stored in FESS while charging")
xlabel("Time [s]")
ylabel("Stored energy [kWh]")
hold on
plot(E2, "LineWidth",2)
plot(E3, "LineWidth",2)
plot(E4, "LineWidth",2)
grid
legend(["r = 0.6 m, m = 1300 kg", "r = 0.6 m, m = 1600 kg", "r =
    0.9 m, m = 1300 kg", "r = 0.9 m, m = 1600 kg"], 'Location','
    northwest', 'NumColumns',2)
ylim([0 90])
```

```
hold off

%Plotting speed of FESSs
plot(n1, "LineWidth",2)
title("Rotor speed of FESS while charging")
xlabel("Time [s]")
ylabel("Rotor speed [rpm]")
hold on
plot(n2, "LineWidth",2)
plot(n3, "LineWidth",2)
plot(n4, "LineWidth",2)
grid
legend(["r = 0.6 m, m = 1300 kg", "r = 0.6 m, m = 1600 kg", "r = 0.9 m, m = 1300 kg", "r = 0.9 m, m = 1600 kg"], 'Location','northwest', 'NumColumns',2)
ylim([0 11000])
hold off

%----------- Charging function---------
function L_new = dpdt(L, I, T, R)
    n_rated = 9000; %Rated speed of FESSs
    p_test = L + (T - R*L/I);

    n = p_test/I * (60/(2*pi));
    if n > n_rated %rated speed
        L_new = n_rated * I /(60/(2*pi));
    elseif n < 0 % Stop
        L_new = 0;
    else
        L_new = p_test;
    end
end
```

B Appendix B: Different electrical machines code

```
close all; clear; clc;

%Flywheel:
r = 0.6; %radius
m = 1300; %mass
I = 0.5*m*r^2; %Moment of inertia

%Machine 1: PMSM
n_rated1 = 7000;
T_rated1 = 228;

%Machine 2: PMSM
n_rated2 = 3000;
T_rated2 = 300;

%Machine 3: IM (Constant n_s)
n_s = 12000;
w_s = n_s * 60/(2*pi);

%Machine 4: VRM
n_base1 = 5000;
n_base2 = 9000;
T_rated4 = 280;

L1=[0];L2=[0];L3=[0];L4=[0]; %Initial angular momentum

%Charing FESS for 2500 seconds with different machines
for i = 1:2500
    L1(end + 1) = PMSM(L1(end), I, T_rated1, n_rated1);
    L2(end + 1) = PMSM(L2(end), I, T_rated2, n_rated2);
    L3(end + 1) = IM(L3(end), I, n_s);
    L4(end + 1) = VRM(L4(end), I, T_rated4, n_base1, n_base2);
end

%Calculating energy and speed of FESS
E1 = 0.5.*(L1.^2)./I .* (2.7778 *10^(-7));
n1 = L1./I .* (60/(2*pi));

E2 = 0.5.*(L2.^2)./I .* (2.7778 *10^(-7));
n2 = L2./I .* (60/(2*pi));

E3 = 0.5.*(L3.^2)./I .* (2.7778 *10^(-7));
n3 = L3./I .* (60/(2*pi));

E4 = 0.5.*(L4.^2)./I .* (2.7778 *10^(-7));
```

```
n4 = L4./I .* (60/(2*pi));

%Plotting energy stored in FESS
plot(E1, "LineWidth",2)
title("Energy stored in FESS")
ylabel("Energy stored [kWh]")
xlabel("Time [s]")
hold on
plot(E2, "LineWidth",2)
plot(E3, "LineWidth",2)
plot(E4, "LineWidth",2)
hold off
legend(["PMSM 1", "PMSM 2", "IM", "VRM"], "Location","northwest")
grid
xlim([0 2200])
ylim([0 55])

%Plotting speed of FESS
plot(n1, "LineWidth",2)
title("Rotational speed of FESS")
ylabel("Rotational speed [RPM]")
xlabel("Time [s]")
hold on
plot(n2, "LineWidth",2)
plot(n3, "LineWidth",2)
plot(n4, "LineWidth",2)
hold off
legend(["PMSM 1", "PMSM 2", "IM", "VRM"], "Location","northwest")
grid
xlim([0 2200])
ylim([0 13000])

%--------PMSM function----------
function L_new = PMSM(L, I, T, n_rated)
    R = 0.0000001;
    n_max = 12000;

    n = L/I * (60/(2*pi));
    if n < n_rated
        L_test = L + (T - R*L/I);
        n = L_test/I * (60/(2*pi));
        if n < 0 % Stop
            L_new = 0;
        else
            L_new = L_test;
        end
    else
```

```
            T_new = (T*n_rated)/n;
            L_test = L + (T_new - R*L/I);
            n = L_test/I * (60/(2*pi));
            if n > n_max %max speed
                L_new = n_max * I /(60/(2*pi));
            else
                L_new = L_test;
            end
        end

end

%--------VRM function----------
function L_new = VRM(L, I, T, n_base1 , n_base2)
    R = 0.0000001;
    n_max = 12000;

    n = L/I * (60/(2*pi));
    if n < n_base1
        L_test = L + (T - R*L/I);
        n = L_test/I * (60/(2*pi));
        if n < 0 % Stop
            L_new = 0;
        else
            L_new = L_test;
        end
    elseif n < n_base2
        T_new = (T*n_base1)/(n);
        L_new = L + (T_new - R*L/I);
    else
        T2 = T*n_base1/n_base2;
        T_new = (T2*n_base2^2)/(n^2);
        L_test = L + (T_new - R*L/I);
        n = L_test/I * (60/(2*pi));
        if n > n_max %max speed
            L_new = n_max * I /(60/(2*pi));
        else
            L_new = L_test;
        end
    end
end

%--------IM function----------
function L_new = IM(L, I, ns)
    R = 0.0000001;
    n = L/I * (60/(2*pi));
    ws = ns* ((2*pi)/60);
```

```
    s = 1 - n/ns;
    Vth = 1.5*224.65;
    R2 = 0.05;
    Rth = 0.1;
    Xth = 0.2;
    X2 = 0.15;
    T = (3 * Vth^2 * R2/s)/(ws*((Rth + R2/s)^2 + (Xth + X2)^2));
    L_new = L + (T - R*L/I);

end
```

C Appendix C: Spin out time and losses code

```
close all; clear; clc;

%FESS
r = 0.6; %radius [m]
m = 1300; %mass [kg]
I = 0.5*m*r^2;

%------------Different C------------
%Losses
A = 0;
B = 0;
C = [0.001, 0.0005, 0.0001, 0.00005, 0.00001, 0.00005];

n_init = 10000; %Initial rotational speed
L_init = n_init * (2*pi/60) * I; %Initial angular momentum
L1 = [L_init];L2 = [L_init];L3 = [L_init];L4 = [L_init];L5 = [
    L_init];L6 = [L_init];

%Letting the FESS spin out
for i = 1:60*60*24*31
    L1(end +1) = dLdt(L1(end), I, 0, A, B, C(1));
    L2(end +1) = dLdt(L2(end), I, 0, A, B, C(2));
    L3(end +1) = dLdt(L3(end), I, 0, A, B, C(3));
    L4(end +1) = dLdt(L4(end), I, 0, A, B, C(4));
    L5(end +1) = dLdt(L5(end), I, 0, A, B, C(5));
    L6(end +1) = dLdt(L6(end), I, 0, A, B, C(6));
end

%Calculating energy stored in FESS
E1 = 0.5.*(L1.^2)./I .* (2.7778 *10^(-7));
E2 = 0.5.*(L2.^2)./I .* (2.7778 *10^(-7));
E3 = 0.5.*(L3.^2)./I .* (2.7778 *10^(-7));
E4 = 0.5.*(L4.^2)./I .* (2.7778 *10^(-7));
E5 = 0.5.*(L5.^2)./I .* (2.7778 *10^(-7));
E6 = 0.5.*(L6.^2)./I .* (2.7778 *10^(-7));

%Plotting energy stored in FESS
x = (0:1/(60*60*24):31);
plot(x, E1, "LineWidth",2, "Color","#0072BD")
hold on
plot(x, E2, "LineWidth",2, "Color","#0072BD")
plot(x, E3, "LineWidth",2, "Color","#0072BD")
plot(x, E4, "LineWidth",2, "Color","#0072BD")
plot(x, E5, "LineWidth",2, "Color","#0072BD")
plot(x, E6, "LineWidth",2, "Color","#0072BD")
```

```
hold off
grid
title("Energy stored in FESS with different C")
ylabel("Energy stored [kWh]")
xlabel("Time [Days]")
xlim([0 31])

%------------Different A------------
%Losses
A = [0.00000001, 0.000000005, 0.000000001, 0.0000000005,
    0.0000000001, 0.00000000005];
B = 0;
C = 0;

%Initial angular momentum
L1 = [L_init];L2 = [L_init];L3 = [L_init];L4 = [L_init];L5 = [
    L_init];L6 = [L_init];

%Letting the FESS spin out
for i = 1:60*60*24*31
    L1(end +1) = dLdt(L1(end), I, 0, A(1), B, C);
    L2(end +1) = dLdt(L2(end), I, 0, A(2), B, C);
    L3(end +1) = dLdt(L3(end), I, 0, A(3), B, C);
    L4(end +1) = dLdt(L4(end), I, 0, A(4), B, C);
    L5(end +1) = dLdt(L5(end), I, 0, A(5), B, C);
    L6(end +1) = dLdt(L6(end), I, 0, A(6), B, C);
end

%Calculating energy in FESS
E1 = 0.5.*(L1.^2)./I .* (2.7778 *10^(-7));
E2 = 0.5.*(L2.^2)./I .* (2.7778 *10^(-7));
E3 = 0.5.*(L3.^2)./I .* (2.7778 *10^(-7));
E4 = 0.5.*(L4.^2)./I .* (2.7778 *10^(-7));
E5 = 0.5.*(L5.^2)./I .* (2.7778 *10^(-7));
E6 = 0.5.*(L6.^2)./I .* (2.7778 *10^(-7));

%Plotting energy stored in FESS
x = (0:1/(60*60*24):31);
plot(x, E1, "LineWidth",2, "Color","#0072BD")
hold on
plot(x, E2, "LineWidth",2, "Color","#0072BD")
plot(x, E3, "LineWidth",2, "Color","#0072BD")
plot(x, E4, "LineWidth",2, "Color","#0072BD")
plot(x, E5, "LineWidth",2, "Color","#0072BD")
plot(x, E6, "LineWidth",2, "Color","#0072BD")
hold off
grid
```

```
title("Energy stored in FESS with different A")
ylabel("Energy stored [kWh]")
xlabel("Time [Days]")
xlim([0 31])

%------------Different B------------
%Losses
A = 0;
B = [0.000001, 0.0000005, 0.0000001, 0.00000005, 0.00000001,
    0.00000005];
C = 0;

%Initial angular momentum
L1 = [L_init];L2 = [L_init];L3 = [L_init];L4 = [L_init];L5 = [
    L_init];L6 = [L_init];

%Letting the FESS spin out
for i = 1:60*60*24*31
    L1(end +1) = dLdt(L1(end), I, 0, A, B(1), C);
    L2(end +1) = dLdt(L2(end), I, 0, A, B(2), C);
    L3(end +1) = dLdt(L3(end), I, 0, A, B(3), C);
    L4(end +1) = dLdt(L4(end), I, 0, A, B(4), C);
    L5(end +1) = dLdt(L5(end), I, 0, A, B(5), C);
    L6(end +1) = dLdt(L6(end), I, 0, A, B(6), C);
end

E1 = 0.5.*(L1.^2)./I .* (2.7778 *10^(-7));
E2 = 0.5.*(L2.^2)./I .* (2.7778 *10^(-7));
E3 = 0.5.*(L3.^2)./I .* (2.7778 *10^(-7));
E4 = 0.5.*(L4.^2)./I .* (2.7778 *10^(-7));
E5 = 0.5.*(L5.^2)./I .* (2.7778 *10^(-7));
E6 = 0.5.*(L6.^2)./I .* (2.7778 *10^(-7));

x = (0:1/(60*60*24):31);
plot(x, E1, "LineWidth",2, "Color","#0072BD")
hold on
plot(x, E2, "LineWidth",2, "Color","#0072BD")
plot(x, E3, "LineWidth",2, "Color","#0072BD")
plot(x, E4, "LineWidth",2, "Color","#0072BD")
plot(x, E5, "LineWidth",2, "Color","#0072BD")
plot(x, E6, "LineWidth",2, "Color","#0072BD")
hold off
grid
title("Energy stored in FESS with different B")
ylabel("Energy stored [kWh]")
xlabel("Time [Days]")
xlim([0 31])
```

```
%--------FESS function---------
function L_new = dLdt(L, I, e0, A, B, C)
    omega = L/I;
    R = A*omega^2 + B*omega + C;
    L_test = L + (e0 - R*L/I);
    n = L_test/I * (60/(2*pi));
    if n < 0 % Stop
        L_new = 0;
    else
        L_new = L_test;
    end
end
```

D Appendix D: Peak shaving code

```
close all; clear; clc

%Flywheel parameters
m = 1300;                   %Mass of flywheel rotor [kg]
r = 0.6;                    %Radius of flywheel rotor [m]
I = 0.5*m*r^2;              %Moment of inertia for flywheel rotor [kg
    *m^2]

n_flywheel_init = 8000; %Initial rotor speed [RPM]
L = [n_flywheel_init*I/((60/(2*pi)))]; %Initial angular momentum

%-------------1 day:-------------

%Time from 00:01 to 23:59
demand_hourly = 2.*[60 40 35 30 30 30 40 80 102 123 130 135 110
    112 125 140 150 160 145 122 107 85 70 65 60]; %W
demand_seconds = [];
%Interpolating to find power demand for every second
for i = 1:(length(demand_hourly)-1)
    for k = 1:3600
        demand_seconds((i-1)*(60*60) + k) = demand_hourly(i) + (
            demand_hourly(i+1) - demand_hourly(i))/3600 * k;
    end
end

%Shaving of the peaks
P_shaved = [];
for i = 1:length(demand_seconds)
    [L(end + 1), P_shaved(end + 1)] = FESS(L(end), I,
        demand_seconds(i));
end

%Power balance to find power on the grid
P_grid = demand_seconds + P_shaved;

%Plotting power on grid
x_axis = [0:1/3600:24]; x_axis = x_axis(1:86400);
plot(x_axis, demand_seconds, "LineWidth",2)
hold on
plot(x_axis, P_grid, "LineWidth",2)
ylim([0 350])
xlim([0 24])
hold off
grid
legend(["Without peak shaving", "With peak shaving"], 'Location',
```

```
    'northwest')
title("Power drawn from grid")
xlabel("Time [Hours]")
ylabel("Power [W]")

%Energy in flywheel
E_flywheel = 0.5.*(L.^2)./I .* (2.7778 *10^(-7));
E_flywheel = E_flywheel(1:86400);

%Plotting energy on grid
plot(x_axis, E_flywheel, "LineWidth",2)
grid
title("Energy stored in FESS")
xlabel("Time [Hours]")
ylabel("Energy [kWh]")
xlim([0 24])
ylim([22.7 23.1])

%-------------1 month:-------------
n_flywheel_init = 8000; %Initial rotor speed [RPM]
L = [n_flywheel_init*I/((60/(2*pi)))]; %Initial angular momentum

%creating a random model for energy demand throughout a month
demand_month = [];
for i = 1:31
    demand_month = cat(2, demand_month, 1.7*rand(1,1).*
       demand_seconds);
end

%Shaving of the peaks
P_shaved = [];
for i = 1:length(demand_month)
    [L(end + 1), P_shaved(end + 1)] = FESS(L(end), I,
       demand_month(i));
end

%Calculating energy on grid
P_grid = demand_month + P_shaved;

%Plotting energy on grid
x_axis = [0:(1/(24*60*60)):32]; x_axis = x_axis(1:2678400);
plot(x_axis, demand_month, "LineWidth",2)
hold on
plot(x_axis, P_grid, "LineWidth",2)
ylim([0 600])
xlim([0 31])
hold off
```

```
grid
legend(["Without peak shaving", "With peak shaving"], 'Location',
    'northwest')
title("Power drawn from grid")
xlabel("Time [Days]")
ylabel("Power [W]")

%Energy in flywheel
E_flywheel = 0.5.*(L.^2)./I .* (2.7778 *10^(-7));
E_flywheel = E_flywheel(1:2678400);

%Plotting energy in flywheel
plot(x_axis, E_flywheel, "LineWidth",2)
grid
title("Energy stored in FESS")
xlabel("Time [Days]")
ylabel("Energy [kWh]")
xlim([0 31])

%-------------FESS function-------------
function [L_new, P_flywheel] = FESS(L, I, P_demand)
    %Motor characteristics
    n_rated = 10000;
    T_rated = 228;
    R = 0.0000001;
    eta = 0.93;
    %Shaving limits
    lower_lim = 100;
    upper_lim = 250;

    if P_demand > upper_lim
        P_needed_el = P_demand - upper_lim;
    elseif P_demand < lower_lim
        P_needed_el = P_demand - lower_lim;
    else
        P_needed_el = 0;
    end
    P_avaliabel = T_rated*p/I; %Mechanical power avaliable

    if P_needed_el < 0 %Generator mode
        P_needed = (P_needed_el) / eta; %Mechanical power needed
            to meet demand
        efficiency_out = eta;
    elseif P_needed_el > 0 %Motoring mode
        P_needed = (P_needed_el) * eta ; %Mechanical power needed
            to meet demand
        efficiency_out = 1/eta;
```

```
    else
        P_needed = 0;
        efficiency_out = 0;
    end

    if P_needed == 0
        T = 0;
        L_test = L - R*L/I;
        n = L_test/I * (60/(2*pi));
        if n < 0 % Rotor stopped
            L_new = 0;
            P_flywheel = 0;
        else
            L_new = L_test;
            P_flywheel = 0;
        end
    elseif abs(P_needed) < P_avaliabel
        T = -P_needed/(p/I);
        L_test = p + (T - R*p/I);
        n = L_test/I * (60/(2*pi));
        if n > n_rated %rated speed
            L_new = n_rated * I /(60/(2*pi));
            P_flywheel = 0;
        elseif n < 0 % Rotor stopped
            L_new = 0;
            P_flywheel = 0;
        else
            L_new = L_test;
            P_flywheel = -P_needed * efficiency_out; %Electric power deliverd to/from flywheel
        end
    else
        L_test = L + (-T_rated - R*L/I);
        n = L_test/I * (60/(2*pi));
        if n > n_rated %rated speed
            L_new = n_rated * I /(60/(2*pi));
            P_flywheel = 0;
        elseif n < 0 % Rotor stopped
            L_new = 0;
            P_flywheel = 0;
        else
            L_new = L_test;
            P_flywheel = -P_avaliabel * efficiency_out; %Electric power deliverd to/from flywheel
        end
    end
end
```

E Appendix E: Specific power output code

```
close all; clear; clc;

%Importing wind data
%Wind speeds from 1. jan - 31. jan 2023 measured in Trondheim
V = readtable("vind1-31jan.csv", "delimiter", ";",'PreserveVariableNames',true);
V = V.Middelvind;
V = replace(V, ",", ".");
V = char(V);
V = str2num(V);
V = V(1:4462);
V = V'; %Wind data for every 10 minutes

%Small-scale wind turbine power
%P at V   [0, 1, 2, 3,  4,   5,   6,   7,    8,    9, 1  0,  11,   12  ]
P_rated = [0, 0, 0, 51, 134, 297, 563, 1000, 1569, 2233, 3064, 3500, 3500];

%Calculates power from wind turbine, for every 10 minutes
P_turbine = [];
for i = 1:length(V)
    P_turbine(i) = P_rated(floor(V(i))+1) + ( P_rated(ceil(V(i))+1) - P_rated(floor(V(i))+1)) * (V(i)-floor(V(i)));
end

%Calculates power from wind turbine, for every seconds
P_turbine_seconds = [];
for i = 1:length(P_turbine)
    for k = 1:(10*60)
        P_turbine_seconds((i-1)*(10*60) + k) = P_turbine(i);
    end
end

%Flywheel parameters
m = 1300;               %Mass of flywheel rotor [kg]
r = 0.6;                %Radius of flywheel rotor [m]
I = 0.5*m*r^2;          %Moment of inertia for flywheel rotor [kg*m^2]

%--------Constant power demand-----------
n_flywheel_init = 8000; %Initial rotor speed [RPM]
L = [n_flywheel_init*I/((60/(2*pi)))]; %Initial angualar momentum

%Power balance
```

```
P_wanted = 160;          %Wanted power outpud [W]
P_flywheel = [];         %Electric power from/into the FESS [W]
%Calculates spin and fplywheel power for every second
for i = 1:length(P_turbine_seconds)
    [L(end+1), P_flywheel(end+1)] = FESS(L(end), I, P_wanted, P_turbine_seconds(i));
end

%Grid power
P_grid = P_turbine_seconds + P_flywheel;

%Energy in flywheel
E_flywheel = 0.5.*(L.^2)./I .* (2.7778 *10^(-7));
E_flywheel = E_flywheel(1:2677200);

x_axis = [1:(1/(24*60*60)):32]; x_axis = x_axis(1:2677200);

%Plot of flywheel and turbine power
plot(x_axis,P_turbine_seconds, "LineWidth",1.5)
title("Power sources")
xlabel("Days (1. jan - 31.jan)")
ylabel("Electrc Power [W]")
grid
hold on
plot(x_axis,P_flywheel, "LineWidth",1.5)
legend(["Wind turbine", "FESS"])
xlim([1 31.6667])
hold off

%Plot of stored enery
plot(x_axis,E_flywheel, "LineWidth",1.5)
title("Energy stored in FESS")
xlabel("Days (1. jan - 31.jan)")
ylabel("Energy stored [kWh]")
xlim([1 31.6667])
grid

%Plot of power to the laod
plot(x_axis,P_grid, "LineWidth",1.5)
title("Power output")
xlabel("Days (1. jan - 31.jan)")
ylabel("Electric Power [W]")
ylim([-100 3200])
xlim([1 31.6667])
grid

%--------Fluctuating power demand: 1 day-----------
```

```
demand_hourly = 1.5.*[60 40 35 30 30 30 40 80 102 123 130 135 110
    112 125 140 150 160 145 122 107 85 70 65 60]; %[W]
mean(demand_hourly);

demand_seconds = [];
%Interpolating to find power demand for every second
for i = 1:(length(demand_hourly)-1)
    for k = 1:3600
        %demand_seconds((i-1)*(60*60) + k) =
        demand_seconds((i-1)*(60*60) + k) = demand_hourly(i) + (
            demand_hourly(i+1) - demand_hourly(i))/3600 * k;
    end
end

%Flywheel
n_flywheel_init = 8000; %Initial rotor speed [RPM]
L = [n_flywheel_init*I/((60/(2*pi)))]; %Initial rotational
    velocity


P_flywheel = []; %Electric power from/into the FESS [W]
%Calculates spin and fplywheel power for every second
for i = 1:length(demand_seconds)
    [L(end+1), P_flywheel(end+1)] = FESS(L(end), I,
        demand_seconds(i), P_turbine_seconds(i));
end

%Grid power
P_grid = P_turbine_seconds(1:86400) + P_flywheel;

%Energy in flywheel
E_flywheel = 0.5.*(L.^2)./I .* (2.7778 *10^(-7));
E_flywheel = E_flywheel(1:86400);

x_axis = [0:1/3600:24]; x_axis = x_axis(1:86400);

%Plot of flywheel and turbine power
plot(x_axis,P_turbine_seconds(1:86400), "LineWidth",1.5)
title("Power sources")
xlabel("Time [hours]")
ylabel("Electrc Power [W]")
grid
hold on
plot(x_axis,P_flywheel, "LineWidth",1.5)
legend(["Wind turbine", "FESS"])
xlim([0 24])
hold off
```

```
%Plot of stored enery
plot(x_axis,E_flywheel, "LineWidth",1.5)
title("Energy stored in FESS")
xlabel("Time [hours]")
ylabel("Energy stored [kWh]")
xlim([0 24])
grid

%Plot of power to the laod
plot(x_axis,P_grid, "LineWidth",1.5)
title("Power output")
xlabel("Time [hours]")
ylabel("Electric Power [W]")
ylim([0 250])
xlim([0 24])
grid

%--------Fluctuating power demand: 1 month-----------
demand_month = [];
for i = 1:31
    demand_month = cat(2, demand_month, demand_seconds);
end

demand_month = demand_month(1:2677200);

%Flywheel
n_flywheel_init = 8000; %Initial rotor speed [RPM]
L = [n_flywheel_init*I/((60/(2*pi)))]; %Initial spin


P_flywheel = [];        %Electric power from/into the FESS [W]
%Calculates spin and fplywheel power for every second
for i = 1:length(demand_month)
    [L(end+1), P_flywheel(end+1)] = FESS(L(end), I, demand_month(
        i), P_turbine_seconds(i));
end

%Grid power
P_grid = P_turbine_seconds + P_flywheel;

%Energy in flywheel
E_flywheel = 0.5.*(L.^2)./I .* (2.7778 *10^(-7));
E_flywheel = E_flywheel(1:2677200);

x_axis = [1:(1/(24*60*60)):32]; x_axis = x_axis(1:2677200);
```

```
%Plot of flywheel and turbine power
plot(x_axis,P_turbine_seconds, "LineWidth",1.5)
title("Power sources")
xlabel("Days (1. jan - 31.jan)")
ylabel("Electrc Power [W]")
grid
hold on
plot(x_axis,P_flywheel, "LineWidth",1.5)
legend(["Wind turbine", "FESS"])
xlim([1 31.6667])
hold off

%Plot of stored enery
plot(x_axis,E_flywheel, "LineWidth",1.5)
title("Energy stored in FESS")
xlabel("Days (1. jan - 31.jan)")
ylabel("Energy stored [kWh]")
xlim([1 31.6667])
grid

%Plot of power to the laod
plot(x_axis,P_grid, "LineWidth",1.5)
title("Power output")
xlabel("Days (1. jan - 31.jan)")
ylabel("Electric Power [W]")
ylim([-100 3200])
xlim([1 31.6667])
grid

%--------FESS function-----------
function [L_new, P_flywheel] = FESS(L, I, P_wanted, P_turbine)
    %Motor characteristics
    n_rated = 10000;
    T_rated = 228;
    R = 0.0000001;
    eta = 0.93;

    P_needed_el = P_turbine - P_wanted; % Electric power needed
    P_avaliabel = T_rated*L/I; %Mechanical power avaliable

    if P_needed_el > 0 %Generator mode
        P_needed = (P_turbine - P_wanted) / eta; %Mechanical
           power needed to meet demand
        efficiency_out = eta;
    else %Motoring mode
        P_needed = (P_turbine - P_wanted) * eta ; %Mechanical
           power needed to meet demand
```

```
            efficiency_out = 1/eta;
        end

        if P_needed < P_avaliabel
            T = P_needed/(L/I);
            L_test = L + (T - R*L/I);
            n = L_test/I * (60/(2*pi));
            if n > n_rated %rated speed
                L_new = n_rated * I /(60/(2*pi));
                P_flywheel = 0;
            elseif n < 0 % Rotor stopped
                L_new = 0;
                P_flywheel = 0;
            else
                L_new = L_test;
                P_flywheel = -P_needed * efficiency_out; %Electric
                   power deliverd to/from flywheel
            end
        else
            L_test = L + (T_rated - R*L/I);
            n = L_test/I * (60/(2*pi));
            if n > n_rated %rated speed
                L_new = n_rated * I /(60/(2*pi));
                P_flywheel = 0;
            elseif n < 0 % Rotor stopped
                L_new = 0;
                P_flywheel = 0;
            else
                L_new = L_test;
                P_flywheel = -P_avaliabel * efficiency_out; %Electric
                    power deliverd to/from flywheel
            end
        end
    end
```

F Appendix F: Frequency control code

```
close all; clear; clc;

%---------- Regulator----------
s = tf('s');
h_fess = exp(-0.0003*s);
h_meter = exp(-0.0003*s);
h_0star = h_fess*h_meter;

bode(h_0star, {1,10000})
set(findall(gcf,'type','line'),'linewidth',2)
grid

%W_wanted at -200 + 45 = 155 degrees
w_wanted = 4500;
amplitude = 0;
T_i = 2.8/w_wanted;
T_d = 1/w_wanted;
Kp = 10^((-amplitude -4 - 28)/20);
n = 10;

h_PID = Kp*((1+T_i*s)/(T_i*s))*((1+T_d*s)/(1+T_d/n*s));
h_0 = h_PID*h_0star;

margin(h_0)
set(findall(gcf,'type','line'),'linewidth',2)
grid

%Plotting step function
h_vy = step(h_meter/(1+h_0),0:0.001:0.5);
plot(h_vy, "LineWidth",2)
xlim([0 200])
grid
title("Step response")
xlabel("Time [ms]")
ylabel("Power balance in system [W]")

%---------- Frequency on grid----------
w_nom = 1500; %Nominal rotational speed of rotor in wind turbine
f_nom = w_nom*4/120; %Frequency at nominal speed

%Flywheel parameters
m = 1300;                  %Mass of flywheel rotor [kg]
r = 0.6;                   %Radius of flywheel rotor [m]
I = 0.5*m*r^2;             %Moment of inertia for flywheel rotor [kg
    *m^2]
```

```

n_flywheel_init = 8000; %Initial rotor speed [RPM]
L = [n_flywheel_init*I/((60/(2*pi)))]; %Initial angular momentum

%Frequency on grid
f_unreg = cat(2, (cat(2,f_nom.*ones(1,200), 1.01*f_nom.*ones
    (1,500))), 0.99*f_nom.*ones(1,500));
f_reg = cat(2, (cat(2,f_nom.*ones(1,200), (0.5.*h_vy(2:501)'+50))
    ), (-h_vy(2:501)'+50));
%Plotting frequencies
plot(f_unreg, "LineWidth",2)
ylim([48 52])
hold on
plot(f_reg, "LineWidth",2)
hold off
ylabel("Frequency [Hz]")
xlabel("Time [ms]")
legend(["No regulation" "Flywheel regulation"])
title("Frequency regulation with FESS")
grid

%Power of wind tubrine and fess
P_wind_nom = 3*10^6; %Production at nominal production
P_load = P_wind_nom;
P_wind = P_wind_nom.*f_unreg./f_nom; %Power from wind (
    proportional to the frequency)
P_FESS = -P_wind_nom.*(f_unreg-f_reg)./f_nom; %Electrical power
    to/from FESS

%Plotting power flows in system
plot((P_wind-P_load)*10^-3, "LineWidth",2)
hold on
plot(P_FESS.*10^-3, "LineWidth",2)
hold off
ylim([-35 45])
title("Power flow in system")
xlabel("Time [ms]")
ylabel("Electric power [kW]")
legend(["P_w_i_n_d - P_l_o_a_d" "P_F_E_S_S_,_e_l"])
grid

%Calculating how the power from the FESS affects the angular
    momentum:
for i = 1:length(P_FESS)
    L(end + 1) = FESS(L(end), I, P_FESS(i));
end

```

```
%Energy stored in FESS
E_FESS = 0.5.*(L.^2)./I .* (2.7778 *10^(-7));
E_FESS = E_FESS(1:1200);

%Plotting energy in FESS
plot(E_FESS, "LineWidth",2)
title("Energy stored in FESS")
xlabel("Time [ms]")
ylabel("Energy stored [kWh]")
%xlim([1 31.6667])
ylim([22.8090 22.815])
grid

%---------- FESS function----------
function L_new = FESS(L, I, P_fess)
    %Motor characteristics
    n_rated = 10000;
    T_rated = 228;
    R = 0.0000001;
    eta = 0.93;

    P_needed_el = P_fess; % Electric power needed
    P_avaliabel = T_rated*L/I; %Mechanical power avaliable

    if P_needed_el > 0 %Generator mode
        P_needed = P_fess / eta; %Mechanical power needed to meet
            demand
    else %Motoring mode
        P_needed = P_fess * eta ; %Mechanical power needed to
            meet demand
    end

    if P_needed < P_avaliabel
        T = P_needed/(L/I);
        L_test = L - (T - R*L/I)*0.001;
        n = L_test/I * (60/(2*pi));
        if n > n_rated %rated speed
            L_new = n_rated * I /(60/(2*pi));
        elseif n < 0 % Rotor stopped
            L_new = 0;
        else
            L_new = L_test;
        end
    else
        L_test = L - (T_rated - R*L/I)*0.001;
        n = L_test/I * (60/(2*pi));
        if n > n_rated %rated speed
```

```
            L_new = n_rated * I /(60/(2*pi));
        elseif n < 0 % Rotor stopped
            L_new = 0;
        else
            L_new = L_test;
        end
    end
end
```

NTNU

Norwegian University of
Science and Technology